Ultrasound for Interventional Pain Management

An Illustrated Procedural Guide

Philip Peng
Roderick Finlayson
Sang Hoon Lee
Anuj Bhatia
Editors

Springer

Ultrasound for Interventional Pain Management

Philip Peng • Roderick Finlayson
Sang Hoon Lee • Anuj Bhatia
Editors

Ultrasound for Interventional Pain Management

An Illustrated Procedural Guide

Springer

Editors
Philip Peng
Department of Anesthesia and Pain Management
Toronto Western Hopsital and Mount Sinai Hospital, University of Toronto
Toronto, Ontario
Canada

Sang Hoon Lee
Madi Pain Management Center
Jeonju, Republic of Korea

Roderick Finlayson
Alan Edwards Pain Management Unit, McGill University Health Centre
Montreal, Quebec
Canada

Anuj Bhatia
Department of Anesthesia and Pain Management
Toronto Western Hopsital and Mount Sinai Hospital, University of Toronto
Toronto, Ontario
Canada

ISBN 978-3-030-18370-7 ISBN 978-3-030-18371-4 (eBook)
https://doi.org/10.1007/978-3-030-18371-4

This Springer imprint is published by the registered company Springer Nature Switzerland AG
The registered company address is: Gewerbestrasse 11, 6330 Cham, Switzerland

This book is dedicated to my wife, Carol, for her continued support, encouragement, and understanding;
to my children, Julia and Michael, who fill me with joy and love;
and to my sister, Rita, who keeps reminding me to be strong and assertive.
Without them, this book would be possible.

Philip Peng

Preface

In the last 15 years, we witnessed a rapid surge in interest in applying ultrasound-guided pain intervention. Before 2003, the interest in ultrasound-guided pain intervention was mostly restricted to musculoskeletal system. Since then, many new techniques in ultrasound-guided pain intervention were developed in various peripheral and axial structures among pain specialists. More recently, the field in musculoskeletal (MSK) pain intervention has entered a renaissance. The MSK pain intervention is not restricted to joint injection any more but also includes fenestration of the tendons/ligaments, barbotage in calcific tendinitis, radiofrequency ablation of articular branches of joints, nonsurgical release of the nerve (e.g., carpal tunnel release), nerve release, and intraneural ablation.

As a result, there are a few books published in the arena of ultrasound-guided pain intervention. So, why did we decide to publish another one?

As our book title suggested, it is an illustrated procedural guide. We have 302 illustrations in 27 chapters. The generous numbers of illustration not just help the readers to grasp the concept of the anatomy and the procedure with ease; it also makes the learning enjoyable. We also make the layout easy and practical. A typical chapter started with an introduction of the procedure, the patient selection, and an overview of anatomy. Then, we presented the step-by-step ultrasound scanning procedure with illustrations. We also summarized all the clinical pearls from the expert. The chapter concluded with a brief review of the literature.

I am honored that three experience clinicians were willing to join me as the section editors: Dr. Anuj Bhatia for the peripheral structures, Dr. Rod Finlayson for the axial structures, and Dr. Sang-Hoon Lee for the musculoskeletal intervention. I sincerely thank them for the team effort. We are indebted to the expert contributors for the tireless effort to compose the chapters and invaluable input of their experience. Our hope is to provide clinicians interested in ultrasound-guided pain intervention an enjoyable learning experience and enrich them with the knowledge to benefit the patients suffering in pain.

Toronto, ON, Canada — Philip Peng
Montreal, QC, Canada — Roderick Finlayson
Jeonju, Republic of Korea — Sang Hoon Lee
Toronto, ON, Canada — Anuj Bhatia

Contents

1 **Basic Principles and Physics of Ultrasound** 1
Sherif Abbas and Philip Peng

2 **Greater and Lesser Occipital Nerve** 33
Yasmine Hoydonckx and Philip Peng

3 **Cervical Sympathetic Trunk** 43
Farah Musaad M. Alshuraim and David Flamer

4 **Suprascapular Nerve** 53
Jay M. Shah, Zachary Pellis, and David Anthony Provenzano

5 **Intercostal Nerve Block** 61
Yu M. Chiu and Amitabh Gulati

6 **Ilioinguinal and Iliohypogastric Nerves** 75
Pranab Kumar and Philip Peng

7 **Genitofemoral Nerve** 83
Athmaja R. Thottungal and Philip Peng

8 **Pelvic Muscles** 93
Anuj Bhatia and Philip Peng

9 **Pudendal and Inferior Cluneal Nerve** 109
Geoff A. Bellingham and Philip Peng

10 **Lateral Femoral Cutaneous Nerve** 121
Ashutosh Joshi and Philip Peng

11 **Erector Spinae Plane Block (ESP Block)** 131
Mauricio Forero, Vicente Roqués, and Nestor Jose Trujillo-Uribe

12 **Ultrasound-Guided Cervical Nerve Root Block** 149
Samer Narouze and Philip Peng

13 **Cervical Medial Branch and Third Occipital Nerve Blocks** 157
John-Paul B. Etheridge and Roderick Finlayson

14 Lumbar Medial Branches and L5 Dorsal Ramus 169
Manfred Greher and Philip Peng

15 Sacroiliac Joint and Sacral Lateral Branch Blocks 185
Roderick Finlayson and María Francisca Elgueta Le-Beuffe

16 Sacroiliac Joint Radiofrequency Ablation 191
Eldon Loh and Robert S. Burnham

17 Caudal Canal Injections 199
Juan Felipe Vargas-Silva and Philip Peng

18 General Principle of Musculoskeletal Scanning and Intervention 207
David A. Spinner and Anthony J. Mazzola

19 Shoulder 213
Jennifer Kelly McDonald and Philip Peng

20 Ultrasound-Guided Injections for Elbow Pain 233
Marko Bodor, Sean Colio, Jameel Khan, and Marc Raj

21 Intervention on Wrist and Hand 247
David A. Spinner and Anthony J. Mazzola

22 Hip 267
Agnes Stogicza

23 Ultrasound-Guided Knee Intervention 283
Thiago Nouer Frederico and Philip Peng

24 Ankle Joint and Nerves 301
Neilesh Soneji and Philip Peng

25 Platelet-Rich Plasma 317
Dmitri Souza

26 Calcific Tendinitis Intervention 325
Sang Hoon Lee

27 Hip and Knee Joint Denervation 335
John Tran and Philip Peng

Index 357

Contributors

Sherif Abbas, MD Department of Anesthesia, UZ Leuven, Leuven, Belgium

Farah Musaad M. Alshuraim, MBBS Department of Anesthesia, Mount Sinai Hospital, Toronto, ON, Canada

Geoff A. Bellingham, MD, FRCPC Department of Anesthesia & Perioperative Medicine, St. Joseph's Health Care London, London, ON, Canada

Anuj Bhatia, MBBS, MD Department of Anesthesia and Pain Management, Toronto Western Hopsital and Mount Sinai Hospital, University of Toronto, Toronto, Ontario, Canada

Marko Bodor, MD Physical Medicine and Rehabilitation, University of California Davis, and Bodor Clinic, Napa, CA, USA

Robert S. Burnham, MSc, MD, FRCPC Central Alberta Pain & Rehabilitation Institute, Lacombe, AB, Canada

Yu M. Chiu, DO Department of Anesthesiology, Division of Pain Medicine, Medical College of Wisconsin, Milwaukee, WI, USA

Sean Colio, MD Bodor Clinic, Napa, CA, USA

John-Paul B. Etheridge, MBChB, DA (SA); CCFP Department of Anesthesia, Kelowna General Hospital, Kelowna, BC, Canada

Roderick Finlayson, MD, FRCPC Alan Edwards Pain Management Unit, McGill University Health Centre, Montreal, Quebec, Canada

David Flamer, MD, FRCPC Anesthesiology and Pain Management, Mount Sinai Hospital – University Health Network, Toronto, ON, Canada

Mauricio Forero, MD, FIPP Department of Anesthesia, McMaster University, Hamilton, ON, Canada

Thiago Nouer Frederico, MD, ASRA-PMUC, WIP-CIPS Department of Anesthesia & Pain, Hospital Sirio Libanes, Sao Paulo, Brazil

Manfred Greher, MD, MBA Department of Anesthesiology, Intensive Care and Pain Therapy, Herz-Jesu Krankenhaus GmbH (Hospital of the Sacred Heart of Jesus), Vienna, Austria

Amitabh Gulati, MD, FIPP CIPS Anesthesiology and Critical Care, Division of Pain Medicine, Memorial Sloan Kettering Cancer Center, New York, NY, USA

Yasmine Hoydonckx, MD, FIPP Department of Anesthesia and Pain Medicine, University of Toronto and Toronto Western Hospital, University Health Network, Toronto, ON, Canada

Ashutosh Joshi, MBBS, MD Department of Anaesthesia, Khoo Teck Puat Hospital, Singapore, Singapore

Jameel Khan, MD Bodor Clinic, Napa, CA, USA

Pranab Kumar, FRCA, FFPMRCA Department of Anesthesia & Pain, Toronto Western Hospital, Toronto, ON, Canada

María Francisca Elgueta Le-Beuffe, MD Department of Anesthesia, Pontificia Universidad Católica de Chile, Santiago, Chile

Sang Hoon Lee, PhD Madi Pain Management Center, Jeonju, Republic of Korea

Eldon Loh, MD, FRCPC Department of Physical Medicine and Rehabilitation, Schulich School of Medicine and Dentistry, Western University, London, ON, Canada

Parkwood Institute, St. Joseph's Health Care London, London, ON, Canada

Anthony J. Mazzola, MD Department of Rehabilitation and Human Performance, Mount Sinai Hospital, New York, NY, USA

Jennifer Kelly McDonald, BScH, MD, FRCPC The Ottawa Hospital, Physical Medicine and Rehabilitation, The Ottawa Hospital Rehabilitation Centre, Ottawa, ON, Canada

Samer Narouze, MD, PhD Center for Pain Medicine, Western Reserve Hospital, Cuyahoga Falls, OH, USA

Zachary Pellis Pain Diagnostics and Interventional Care, Sewickley, PA, USA

Philip Peng, MBBS, FRCPC Department of Anesthesia and Pain Management, Toronto Western Hopsital and Mount Sinai Hospital, University of Toronto, Toronto, Ontario, Canada

David Anthony Provenzano, MD Pain Diagnostics and Interventional Care, Sewickley, PA, USA

Marc Raj, DO Bodor Clinic, Napa, CA, USA

Vicente Roqués Department of Anesthesia, Intensive Care and Pain Treatment, University Hospital Virgen de la Arrixaca, Murcia, Spain

Jay M. Shah, MD SamWell Institute of Pain Management, Woodbridge, NJ, USA

Neilesh Soneji, MD, FRCPC Department of Anesthesia, University of Toronto, Toronto, ON, Canada

Department of Anesthesia and Pain Management, University Health Network – Toronto Western Hospital, Women's College Hospital, Toronto, ON, Canada

Dmitri Souza, MD, PhD Ohio University, Heritage College of Osteopathic Medicine, Athens, OH, USA

Center for Pain Medicine, Western Reserve Hospital, Cuyahoga Falls, OH, USA

David A. Spinner, DO, RMSK, CIPS, FAAPMR Department of Rehabilitation and Human Performance, Mount Sinai Hospital, New York, NY, USA

Agnes Stogicza, MD, FIPP, CIPS Anesthesiology and Pain Management, Saint Magdolna Private Hospital, Budapest, Hungary

Athmaja R. Thottungal, MBBS Department of Anaesthesia & Pain, Kent and Canterbury Hospital, Canterbury, UK

John Tran, HBSc Division of Anatomy, Department of Surgery, 1 King's College Circle, Toronto, ON, Canada

Nestor Jose Trujillo-Uribe, MD Universidad Autónoma de Bucaramanga, Bucaramanga, Colombia

Department of Anesthesia and Pain Medicine, Fundación Oftalmológica de Santander, Clínica Carlos Ardila Lule, Clínica del Dolor y Cuidado Paliativo ALIVIAR LTDA, Floridablanca, Colombia

Juan Felipe Vargas-Silva, MD Department of Surgery and Image Guided Therapy, Pain Clinic, Hospital Pablo Tobón Uribe, Medellin, Colombia

About the Editor

Philip Peng is a full professor in the Department of Anesthesia and Pain Management of the University of Toronto and is currently the director of Anesthesia Pain Program in Toronto Western Hospital and interim director of Wasser Pain Management Center.

He has played an important role in the education of the pain medicine and established major teaching courses for pain in Canada such as the National Pain Refresher Course, Canadian Pain Interventional Course, and Ultrasound for Pain Medicine Course. The Royal College of Physicians and Surgeons of Canada (RCPSC) honored him with founder designation in pain medicine for his role in establishing pain medicine subspecialty in Canada. Besides, he currently serves as the chair of the Exam Committee in Pain Medicine in RCPSC and previously served as the chair of the Education Special Interest Group (SIG) of Canadian Pain Society and the founding executive of Pain Education SIG of International Association for the Study of Pain (IASP). He has been honored with numerous teaching awards at national and regional level.

Dr. Philip Peng is also a leader and pioneer in the application of ultrasound for pain medicine. Being one of the founding fathers for Ultrasound for Pain Medicine (USPM) SIG for ASRA (American Society of Regional Anesthesia), he was involved in the establishment of the guideline for Education and Training for USPM, which was adopted by five continents. He is the chair for the new Ultrasound for Pain Medicine Exam Certificate and chair for the Musculoskeletal Pain Ultrasound Cadaver workshop for ASRA and has been the chair or main organizer for various major teaching courses for USPM, including satellite meeting of the World Congress on Pain, International Pain Congress, combined Canadian and British Pain Society Conference, International Symposium of Ultrasound for Regional Anesthesia (ISURA), and Canadian Pain Interventional Course.

Furthermore, he has edited 7 books and published more than 150 peer-reviewed publications and book chapters.

Basic Principles and Physics of Ultrasound

1

Sherif Abbas and Philip Peng

Understanding the Physics of Ultrasound and Image Generation

Characteristic of Sound Wave

Audible sound wave lies within the range of 20–20,000 Hz. Ultrasound is a sound wave beyond audible range (>20,000 Hz). Ultrasound system commonly used in clinical settings incorporates transducers generating frequencies between 2 and 17 MHz. Some special ultrasound system even generates frequencies between 20 and 55 MHz. Sound waves do not exist in a vacuum, and propagation in gases is poor because the molecules are too widely spaced, which explains the use of gel couplant between the skin of the subject and the transducer interface to eliminate the air-filled gap.

Sound wave is a form of mechanical energy that travels through a conducting medium (e.g., body tissue) as a longitudinal wave producing alternating compression (high pressure) and rarefaction (low pressure) (Figs. 1.1 and 1.2). Sound propagation can be represented in a sinusoidal waveform with a characteristic pressure (P), wavelength (λ), frequency (f), period (T), and velocity. See Table 1.1 for details.

The speed of sound varies for different biological media, but the average value is assumed to be 1540 m/s for most human soft tissues. It can vary greatly, being as low as 330 m/s in air and as high as 4000 m/s through bone.

The wavelength (λ) is inversely related to the frequency (f). Thus, sound with a high frequency has a short wavelength and vice versa.

S. Abbas
Department of Anesthesia, UZ Leuven, Leuven, Belgium

P. Peng (✉)
Department of Anesthesia and Pain Management, Toronto Western Hopsital and Mount Sinai Hospital, University of Toronto, Toronto, Ontario, Canada
e-mail: Philip.peng@uhn.ca

P. Peng et al. (eds.), *Ultrasound for Interventional Pain Management*,
https://doi.org/10.1007/978-3-030-18371-4_1

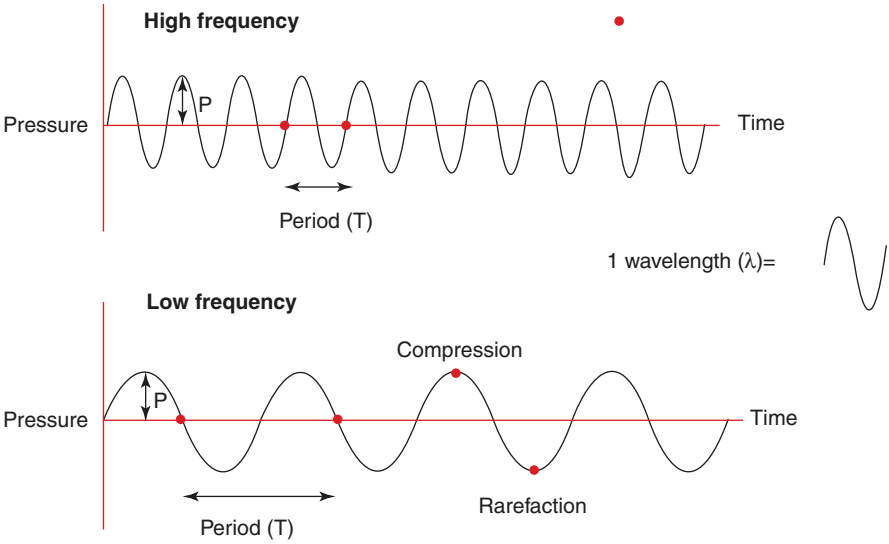

Fig. 1.1 Comparison of high-frequency and low-frequency waveform. (Reprinted with permission from Philip Peng Educational Series)

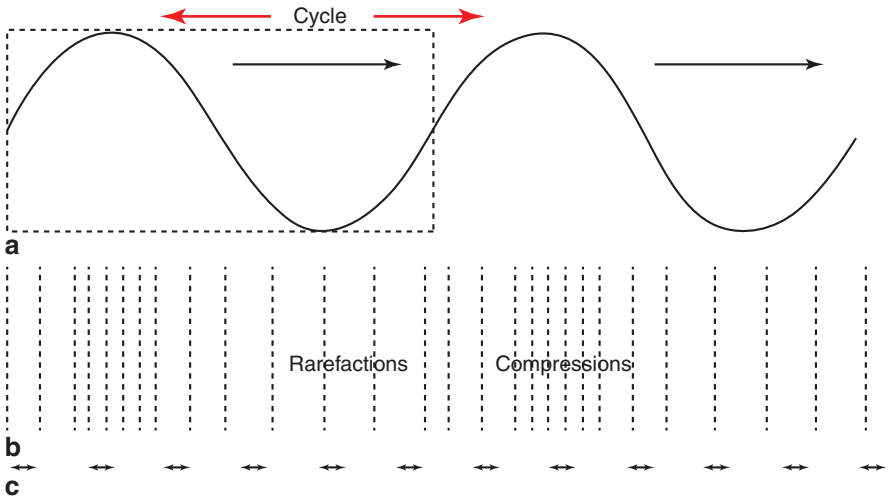

Fig. 1.2 A longitudinal wave showing alternating compression and rarefaction. (Reprinted with permission from Philip Peng Educational Series)

Generation of an Ultrasound Wave

An ultrasound wave is generated when an electric field is applied to an array of piezoelectric crystals located on the transducer surface. Electrical stimulation causes mechanical distortion of the crystals resulting in vibration and production of sound waves (i.e., mechanical energy). The conversion of electrical to mechanical

Table 1.1 Basic terminology

Terminology	Definition
Wavelength (λ)	The spatial period of the wave, and is determined by measuring the distance between two consecutive corresponding points of the same phase. It is expressed in meters (m)
Amplitude (A)	A measure of the height of the wave, i.e., maximal particle displacement. It is expressed in meters (m)
Period (T)	The time taken for one complete wave cycle to occur. The unit of period is seconds (s)
Frequency (f)	The number of completed cycles per second. Thus, it is the inverse of the period (T) of a wave. The unit of frequency is hertz (Hz). Medical imaging uses high-frequency waves (1–20 MHz)
Velocity (c)	The speed of propagation of a sound wave through a medium (m/s). It is the product of its frequency (f) and wavelength (λ)
Energy (E)	The energy of a sound wave is proportional to the square of its amplitude (A). This means that as the amplitude of a wave decreases (such as with deeper penetration), the energy carried by the wave reduces drastically
Power (P)	Defines as the energy (E) delivered per unit time (t)

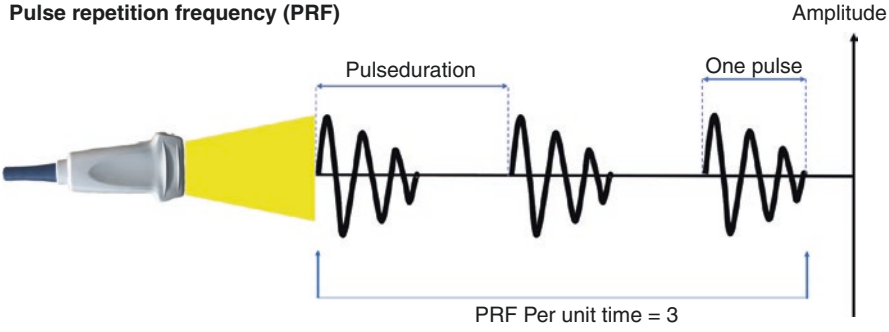

Fig. 1.3 Pulse repetition frequency. (Reprinted with permission from Philip Peng Educational Series)

(sound) energy is called the converse piezoelectric effect. Each piezoelectric crystal produces an ultrasound wave. The summation of all waves generated by the piezoelectric crystals forms the ultrasound beam. Ultrasound waves are generated in pulses (intermittent trains of pressure waves), and each pulse commonly consists of two or three sound cycles of the same frequency.

The pulse length (PL) is the distance traveled per pulse. Waves of short pulse lengths improve axial resolution for ultrasound imaging. The PL cannot be reduced to less than 2 or 3 sound cycles by the damping materials within the transducer.

Pulse repetition frequency (PRF) is the rate of pulses emitted by the transducer (number of pulses per unit time) (Fig. 1.3). Ultrasound pulses must be spaced with enough time between pulses to permit the sound to reach the target of interest and return to the transducer before the next pulse is generated. The PRF for medical imaging ranges from 1 to 10 kHz. For example, if the PRF = 5 kHz and the time between pulses is 0.2 ms, it will take 0.1 ms to reach the target and 0.1 ms to return to the transducer. This means the pulse will travel 15.4 cm before the next pulse is emitted (1540 m/s × 0.1 ms = 0.154 m in 0.1 ms = 15.4 cm).

Generation of an Ultrasound Image

An ultrasound image is generated when the pulse wave emitted from the transducer is transmitted into the body, reflected off the tissue interface, and returned to the transducer. The schematic diagram above showed the transducer waits to receive the returning wave (i.e., echo) after each pulsed wave (Fig. 1.4). The transducer transforms the echo (mechanical energy) into an electrical signal which is processed and displayed as an image on the screen. The conversion of sound to electrical energy is called the piezoelectric effect.

The image can be displayed in a number of modes (Fig. 1.5):

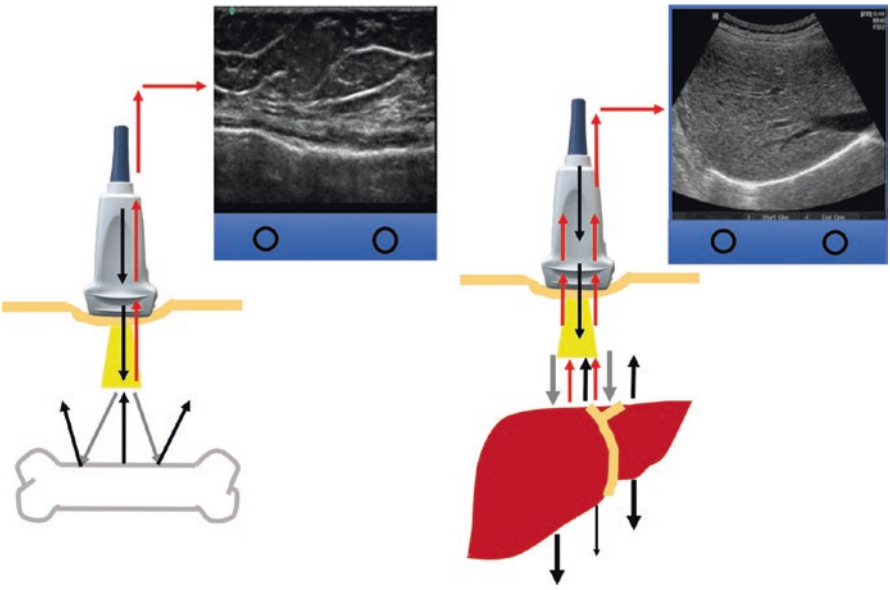

Fig. 1.4 Ultrasound wave interaction with body tissue. (Reprinted with permission from Philip Peng Educational Series)

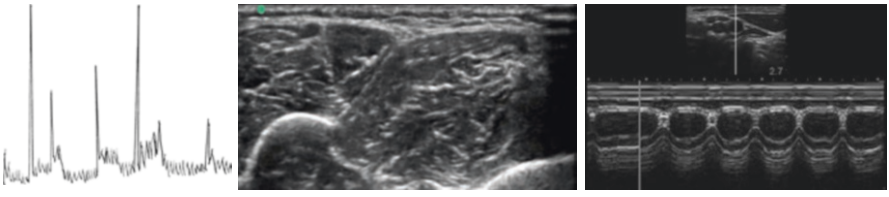

Fig. 1.5 Three different modes of ultrasound. (Reprinted with permission from Philip Peng Educational Series)

- *Amplitude (A)* mode is the display of amplitude spikes in the vertical axis and the time required for the return of the echo in the horizontal axis.
- *Brightness (B)* displays a two-dimensional map of the data acquired and is most commonly used for ultrasound guided intervention.
- *Motion (M)* mode, also called time motion or TM mode, displays a one-dimensional image usually used for analyzing moving body parts. This mode records the amplitude and rate of motion in real time and is commonly used in cardiovascular imaging.

Ultrasound Tissue Interaction

As the ultrasound beam travels through tissue layers, the amplitude of the original signal becomes attenuated as the depth of penetration increases (Fig. 1.6).

Attenuation (energy loss) is due to:

1. Absorption (conversion of acoustic energy to heat)
2. Reflection
3. Scattering at interfaces

In soft tissue, 80% of the attenuation of the sound wave is caused by absorption resulting in heat production. Attenuation is measured in decibels per centimeter of

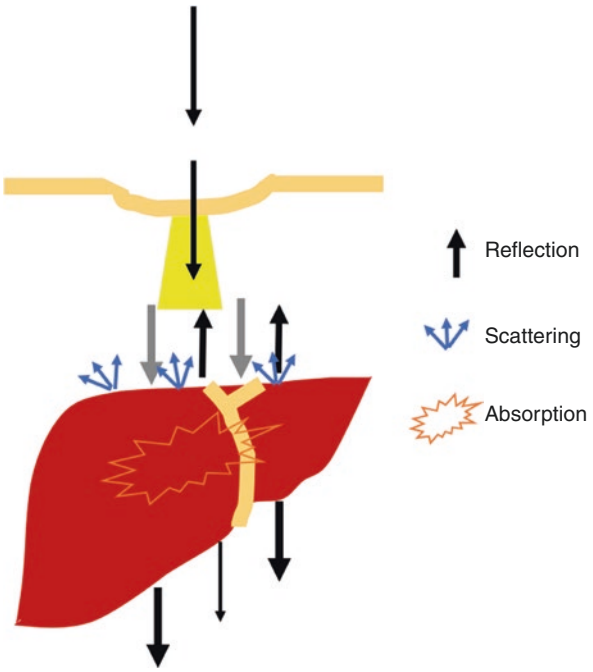

Fig. 1.6 Different types of attenuation. (Reprinted with permission from Philip Peng Educational Series)

tissue and is represented by the attenuation coefficient of the specific tissue type. The higher the attenuation coefficient, the more attenuated the ultrasound wave is by the specified tissue.

Absorption

Absorption is the process of transfer of the ultrasound beam's energy to the medium through which it travels through heat generation and it accounts for most of the wave attenuation. The quality of the returning sound waves depends on the attenuation coefficient of different tissue.

The degree of attenuation also varies directly with the frequency of the ultrasound wave and the distance traveled (Fig. 1.7 and Table 1.2). Generally speaking,

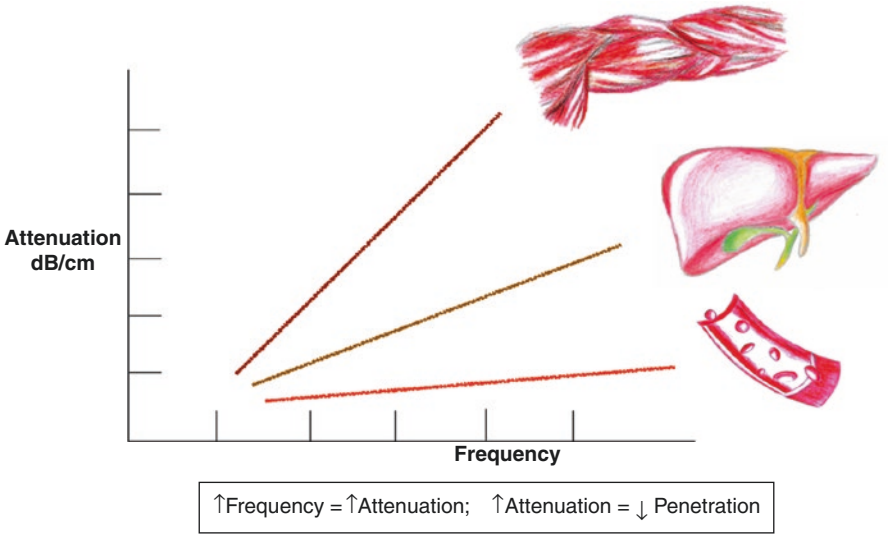

Fig. 1.7 Variation of attenuation with frequency in different organs. (Reprinted with permission from Philip Peng Educational Series)

Table 1.2 Attenuation coefficient of various tissues

Material	α (dB/cm)
Blood	0.18
Fat	0.6
Muscle (across fibers)	3.3
Muscle (along fibers)	1.2
Aqueous and vitreous humor of the eye	0.1
Lens of the eye	2.0
Skull bone	20
Lungs	40
Liver	0.9
Brain	0.85
Kidney	1.0
Spinal cord	1.0
Water	0.0022
Castor oil	0.95
Lucite	2.0

a high-frequency wave is associated with high attenuation, thus limiting tissue penetration, whereas a low-frequency wave is associated with low tissue attenuation and deep tissue penetration.

To compensate for attenuation, it is possible to amplify the signal intensity of the returning echo. The degree of receiver amplification is called the gain. Increasing the gain will amplify only the returning signal and not the transmit signal. An increase in the overall gain will increase brightness of the entire image, including the background noise. Preferably, the time gain compensation (TGC) is adjusted to selectively amplify the weaker signals returning from deeper structures.

Reflection

Attenuation also results from reflection and scattering of the ultrasound wave. The extent of reflection is determined by the difference in acoustic impedances of the two tissues at the interface, i.e., the degree of impedance mismatch.

Acoustic impedance is the resistance of a tissue to the passage of ultrasound. The higher the degree of impedance mismatch, the greater the amount of reflection (Table 1.3). The degree of reflection is high for air because air has an extremely low acoustic impedance (0.0004) relative to other body tissues. The bone also produces a strong reflection because its acoustic impedance is extremely high (7.8) relative to other body tissues. For this reason, it is clinically important to apply sufficient conducting gel (an acoustic coupling medium) on the transducer surface to eliminate any air pockets between the transducer and skin surface. Otherwise, much of the ultrasound waves will be reflected limiting tissue penetration.

The angle of the incidence is also a major determinant of reflection. An ultrasound wave hitting a smooth mirror-like interface at a 90° angle will result in a perpendicular reflection. An incident wave hitting the interface at an angle <90° will result in the wave being deflected away from the transducer at an angle equal to the angle of incidence but in the opposite direction (angle of reflection). When this happens, the signal of the returning echo is weakened, and a darker image is displayed (Fig. 1.8). This explains why it is difficult to visualize a needle inserted at a steep angle (>45° to the skin surface).

Specular reflection occurs at flat, smooth interfaces where the transmitted wave is reflected in a single direction depending on the angle of incidence. Examples of specular reflectors are fascial sheaths, the diaphragm, and walls of major vessels

Table 1.3 Acoustic impendence of various tissues

Body tissue	Acoustic impedance (10^6 RayIs)
Air	0.0004
Lung	0.18
Fat	1.34
Liver	1.65
Blood	1.65
Kidney	1.63
Muscle	1.71
Bone	7.8

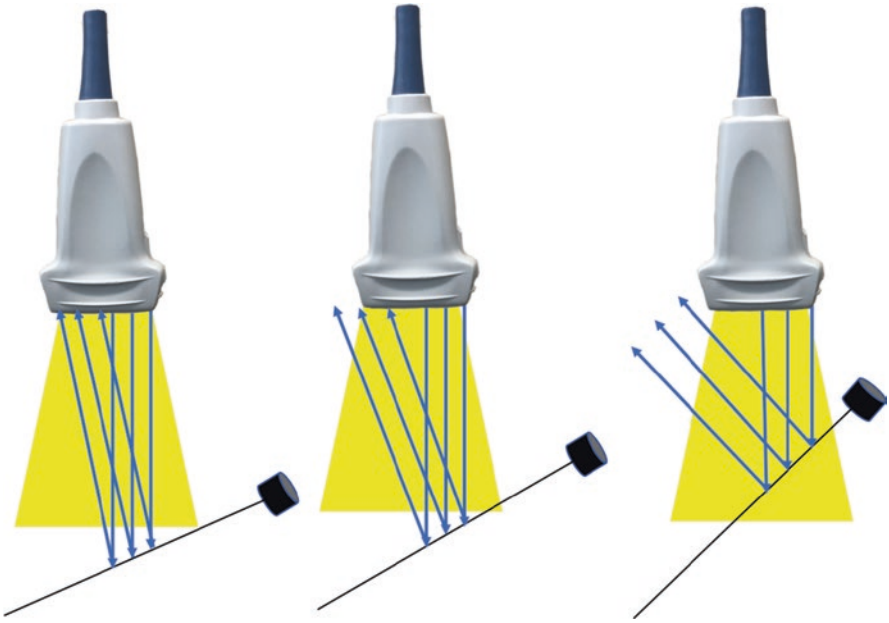

Fig. 1.8 Angle of incidence. (Reprinted with permission from Philip Peng Educational Series)

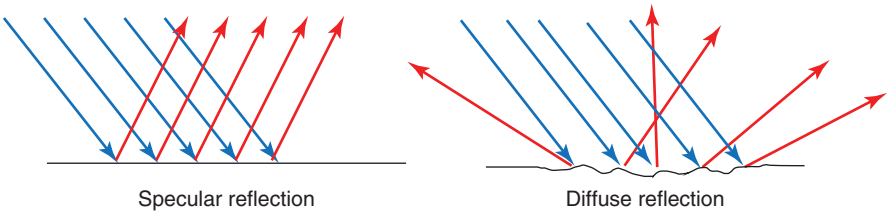

Fig. 1.9 Different types of reflection. (Reprinted with permission from Philip Peng Educational Series)

(Fig. 1.9). Block needles are also strong specular reflectors. For specular reflection to occur, the wavelength of the ultrasound wave must be smaller than the reflective structure. Otherwise, scattering will occur.

Scattering

Reflection in biological tissues is not always specular. Scattering (diffuse reflection) occurs when the incident wave encounters an interface that is not perfectly smooth (e.g., surface of visceral organs). Echoes from diffuse reflectors are generally weaker than those returning from specular reflectors. Scattering also occurs when the wavelength of the ultrasound wave is larger than the dimensions of the reflective structure (e.g., red blood cells). The reflected echo scatters in many different

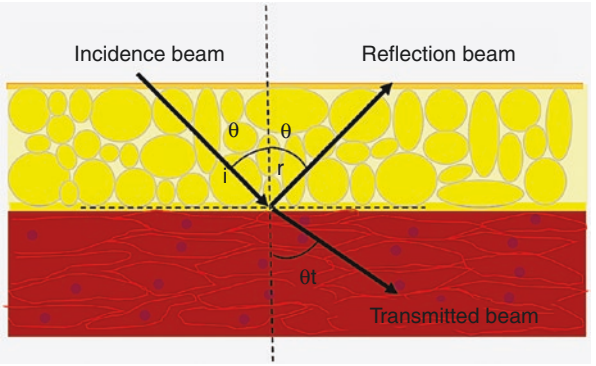

Fig. 1.10 Transmission of beam. (Reprinted with permission from Philip Peng Educational Series)

directions resulting in echoes of similar weak amplitudes. Ultrasonic scattering gives rise to much of the diagnostic information we observe in medical ultrasound imaging.

Transmission

After reflection and scattering, the remainder of the incident beam is refracted with a change in the direction of the transmitted beam (Fig. 1.10). Refraction occurs only when the speeds of sound are different on each side of the tissue interface. The degree of beam change (bending) is dependent on the change in the speed of sound traveling from one medium on the incident side to another medium on the transmitted side (Snell's Law). With medical imaging, fat causes considerable refraction and image distortion, which contributes to some of the difficulties encountered in obese patients. Refraction encountered with bone imaging is even more significant leading to a major change in the direction of the incident beam and image distortion.

The final image on the screen of an ultrasound machine is the result of the interaction of ultrasound waves with the tissues being examined. As the ultrasound wave travels through the tissues, it loses amplitude, and hence energy (attenuation), which is the summative effect of absorption, reflection, and refraction of ultrasound waves.

Image Acquisition and Processing

Transducer Basic

An ultrasound transducer has a dual functionality. It is responsible for both the production of ultrasound waves and, after a set period of time, the reception of waves reflected from the tissues. This is called pulsed ultrasound. The pulse repetition frequency (PRF) is the number of pulses emitted by the transducer per unit of time. The PRF for medical imaging devices ranges from 1 to 10 kHz

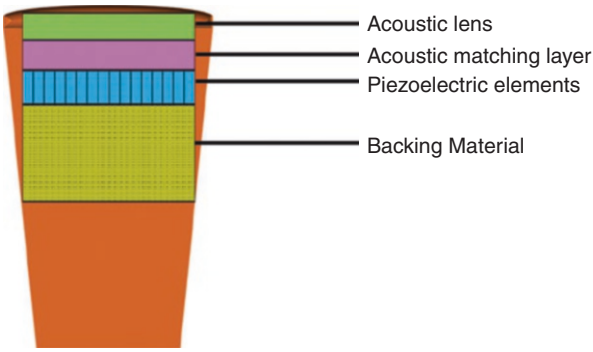

Fig. 1.11 Anatomy of a transducer. (Reprinted with permission from Philip Peng Educational Series)

The ultrasound transducer has the following layers (Fig. 1.11):

(a) Backing material: located behind the piezoelectric element, it serves to prevent excessive vibration. This causes the element to generate ultrasonic waves with a shorter pulse length, improving axial resolution in images.
(b) Piezoelectric elements: they generate ultrasonic waves and also generate images. Piezoelectric ceramic (PZT: lead zirconate titanate) is most commonly used because of their high conversion efficiency.
(c) Acoustic matching layer: this reduces the acoustic impedance mismatch between the transducer and the object and thus minimizes reflection off the interface. This is usually made up of a resin.
(d) Acoustic lens: the acoustic lens prevents the ultrasonic waves from spreading and focuses them in the slice direction to improve the resolution.

Transducer Selection

The choice of which transducer should be used depends on the depth of the structure being imaged. The higher the frequency of the transducer crystal, the less penetration it has but the better the resolution. Therefore, if more penetration is required, you need to use a lower-frequency transducer with the sacrifice of some resolution.

Transducer characteristics, such as frequency and shape, determine ultrasound image quality. For simplicity, there are three types of transducers.

The linear transducer frequencies used for superficial structures and peripheral nerve blocks range from 6 to 15 MHz (Fig. 1.12). Curvilinear (or curved) transducers are most useful for deeper structures or imaging requiring a wide field of view (e.g., spine). Microconvex is commonly used for small acoustic window such as cardiac scanning.

For superficial structures (e.g., nerves in the interscalene region), it is ideal to use high-frequency transducers in the range of 10–15 MHz, but depth of penetration is often limited to 2–3 cm below the skin surface (Fig. 1.13). For visualization of

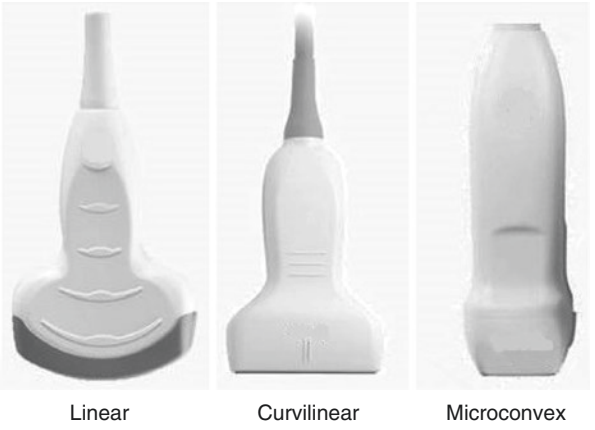

Fig. 1.12 Different types of transducer. (Reprinted with permission from Philip Peng Educational Series)

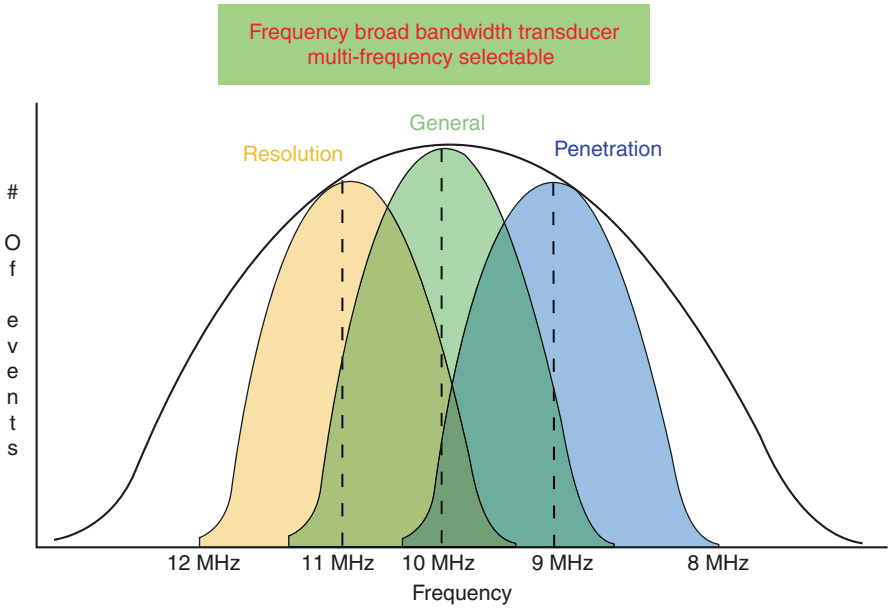

Fig. 1.13 Frequency, resolution, and penetration. (Reprinted with permission from Philip Peng Educational Series)

deeper structures (e.g., in the gluteal region) or when a wider field of view is required, it may be necessary to use a lower-frequency transducer (2–5 MHz) because it offers ultrasound penetration of 4–5 cm or more below the skin surface. However, the image resolution is often inferior to that obtained with a higher-frequency transducer.

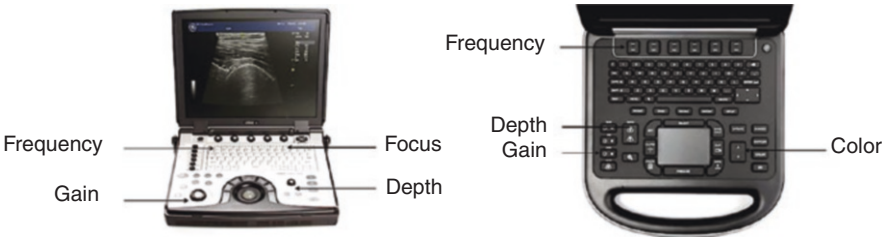

Fig. 1.14 Basic button of ultrasound machine. (Reprinted with permission from Philip Peng Educational Series)

Basic Operation of Ultrasound Machine

To obtain a good ultrasound picture, clinician should be familiar with the basic function and buttons in the ultrasound machine: gain, depth, color (Doppler), and focus (Fig. 1.14).

Gain

The echo signals returning from the tissues reach the crystals and produce an electric current (piezoelectric effect). This is then converted to a pixel on the image, with the energy of the returning wave being proportional to the brightness of the pixel dot on the image. The amplitude of the returning echo signals is very small to be properly displayed on a screen. Hence, it needs amplification. Amplification of signal can be adjusted using the GAIN button, but the use of it adds to "background noise."

Time gain compensation It is the preferential enhancement of signals at different depths returning from deeper tissues (Fig. 1.15). Thus, the echoes returning from similar reflectors can be represented by the same shade of gray regardless of their depth.

Depth

The depth of the field should be adjusted to the area of interest (Fig. 1.16). Too shallow may miss the important information from the background in the deep field, and too deep will diminish the quality of the image in the superficial field.

Focus

The shape of the beam varies and is different for each transducer frequency. There is a fixed focused region of the ultrasound beam which is indicated on the system with a small triangle to the right of the image. This indicates the focal zone of that

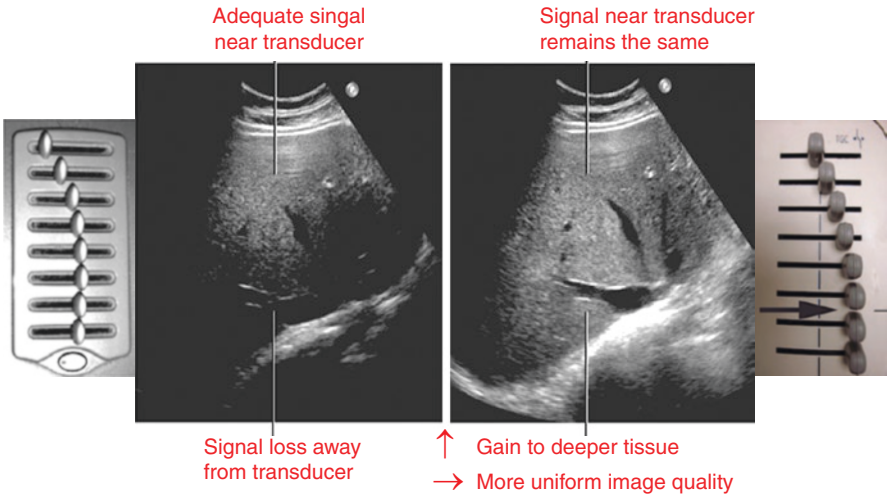

Fig. 1.15 Time gain compensation. (Reprinted with permission from Philip Peng Educational Series)

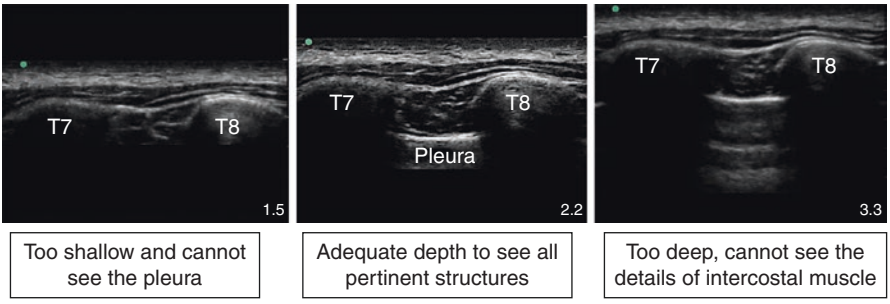

Fig. 1.16 Depth and image acquired. (Reprinted with permission from Philip Peng Educational Series)

transducer and is where the best resolution can be achieved with that particular transducer (Fig. 1.17). Effort should be taken to position the object of interest in the subject to within that focused area to obtain the best detail by adjusting the FOCUS button (Fig. 1.18).

Doppler

The Doppler information is displayed graphically using spectral Doppler, or as an image using color Doppler (directional Doppler) or power Doppler (non-directional Doppler).

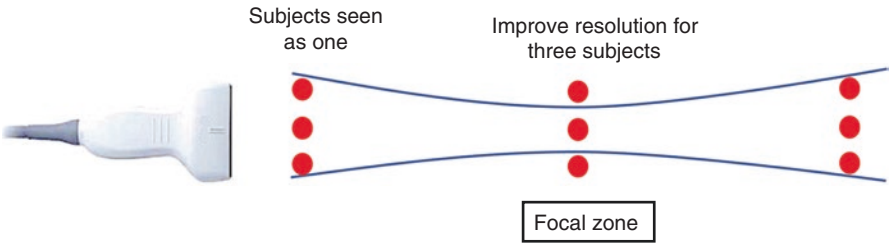

Fig. 1.17 Focus of a beam. (Reprinted with permission from Philip Peng Educational Series)

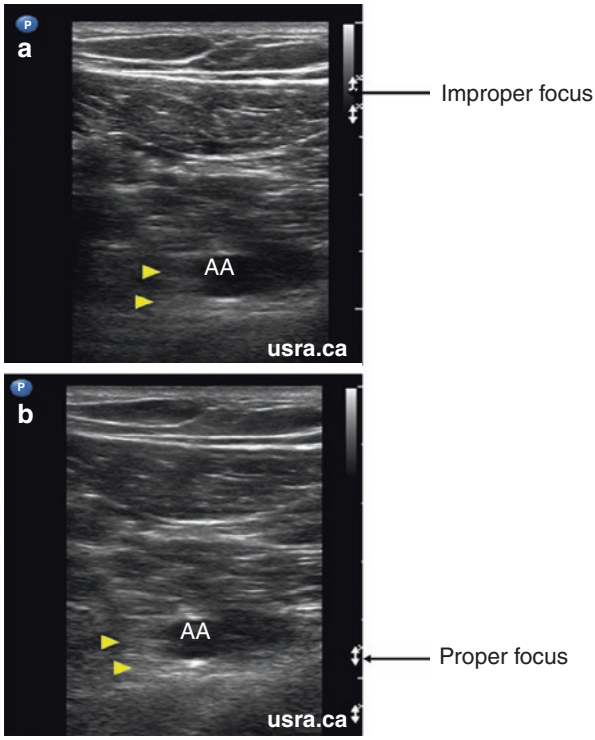

Fig. 1.18 Effect of focus setting and image acquired. (Reprinted with permission from usra.ca)

All modern ultrasound scanners use pulsed Doppler to measure velocity. Pulsed wave machines transmit and receive series of pulses.

In color Doppler, echoes are displayed with colors corresponding to the direction of flow that their positive or negative Doppler shifts represent (toward or away from the transducer). The brightness of the color represents the intensity of the echoes, and sometimes other colors are added to indicate the extent of spectral broadening (Fig. 1.19).

Power Doppler depicts the amplitude or power of Doppler signals rather than the frequency shift. This allows detection of a larger range of Doppler shifts and therefore better visualization of the smaller vessels, but at the expense of directional and velocity information.

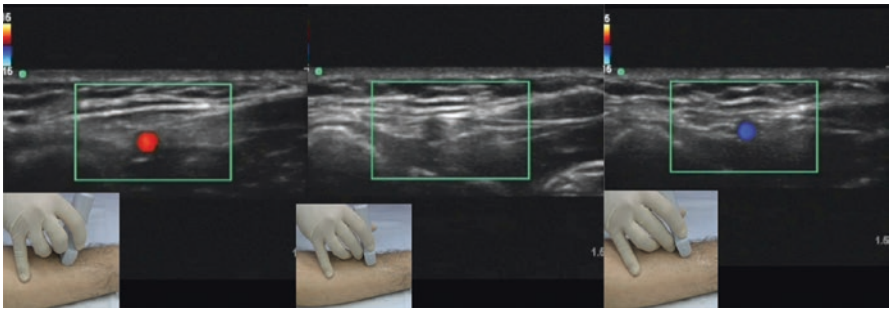

Fig. 1.19 Color Doppler. (Reprinted with permission from Philip Peng Educational Series)

Understanding Sonoanatomy and Artifact

Tissue Echogenicity

When an echo returns to the transducer, its amplitude is represented by the degree of brightness (i.e., echogenicity) of a dot on the display. Combination of all the dots forms the final image. Strong specular reflections give rise to bright dots (hyperechoic), e.g., the diaphragm, gallstone, bone, and pericardium. Weaker diffuse reflections produce gray dots (hypoechoic), e.g., solid organs. No reflection produces dark dots (anechoic), e.g., fluid- and blood-filled structures, because the beam passes easily through these structures without significant reflection. Also, deep structures often appear hypoechoic because attenuation limits beam transmission to reach the structures, resulting in a weak returning echo.

Sonoanatomic Features of Tissue

Vessels

Left sonogram showed a round anechoic artery (A) and an oval-shaped anechoic vein (V) (Fig. 1.20). An artery is pulsatile and not easily compressible. A vein is collapsible and non-pulsatile. Figure 1.21 showed the long axis of vessels with color Doppler on. As discussed in the above section, red color indicates the direction of flow and does not confirm the presence of an artery.

The Adipose, Muscle, and Bone

The left sonogram showed the typical appearance of adipose tissue, which is hypoechoic background with streaks of hyperechoic lines that are often irregular in texture and length (Fig. 1.22). Appearance of muscle is generally hypoechoic. The structure deep to the adipose tissue is the rectus muscle in transverse plane, which has a speckled appearance. The sonogram on the right displayed the muscle in long

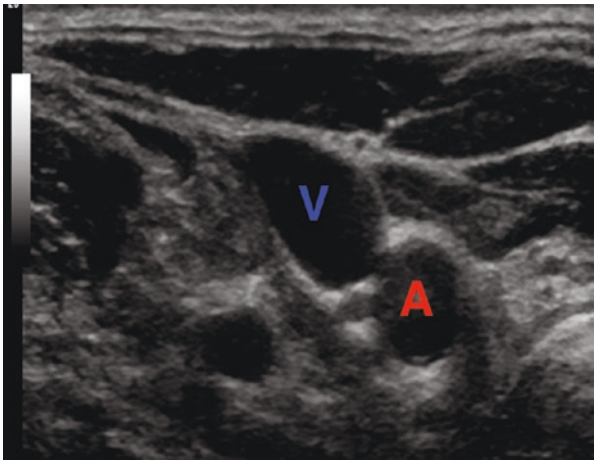

Fig. 1.20 Sonoanatomy of vessels. (Reprinted with permission from Philip Peng Educational Series)

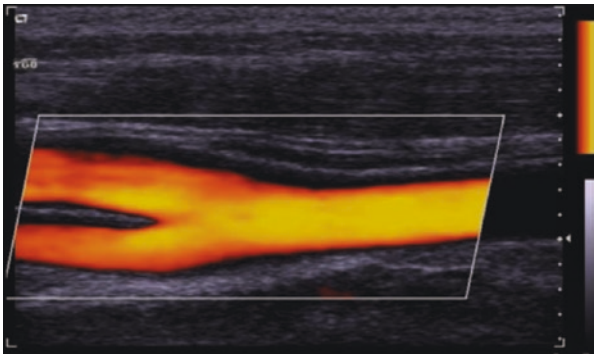

Fig. 1.21 Vessel with color Doppler on. (Reprinted with permission from Philip Peng Educational Series)

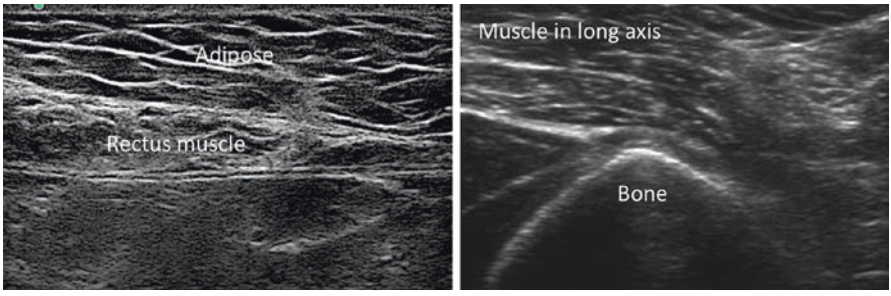

Fig. 1.22 Sonoanatomy of the muscle, adipose tissue, and bone. (Reprinted with permission from Philip Peng Educational Series)

axis, and the perimysial connective tissue is apparent in linear pattern. The bone appears as an hyperechoic line with an anechoic shadow due to lack of beam penetration.

Nerve

The appearance of the nerve (yellow arrows) can be hyperechoic, hypoechoic, or mixed, depending on the location, size, amount of connective tissue, and the angle of the transducer (Fig. 1.23). Above the clavicle, the nerve roots typically appear as hypoechoic (left upper sonogram). As the peripheral nerve picks up more connective tissues, it appears as hyperechoic (femoral nerve in the right upper sonogram). A peripheral nerve can also appear as mixed hyper- and hypoechoic (honeycomb appearance) as shown in the left lower sonogram. In long axis, the nerve appears hypoechoic with fibrillar pattern in the right lower sonogram. However, compared with the tendon in long axis (right sonogram in Fig. 1.24 below), the nerve is more hypoechoic, and the echotexture is coarse.

Tendon

The left sonogram showed the tendon in short axis, which showed densely fibrillar pattern (Fig. 1.24). Comparison of the long axis view of the tendon in the right sonogram with that of the nerve in Fig. 1.23 (right lower sonogram) shows that the tendon is more echogenic and fibrillar in appearance.

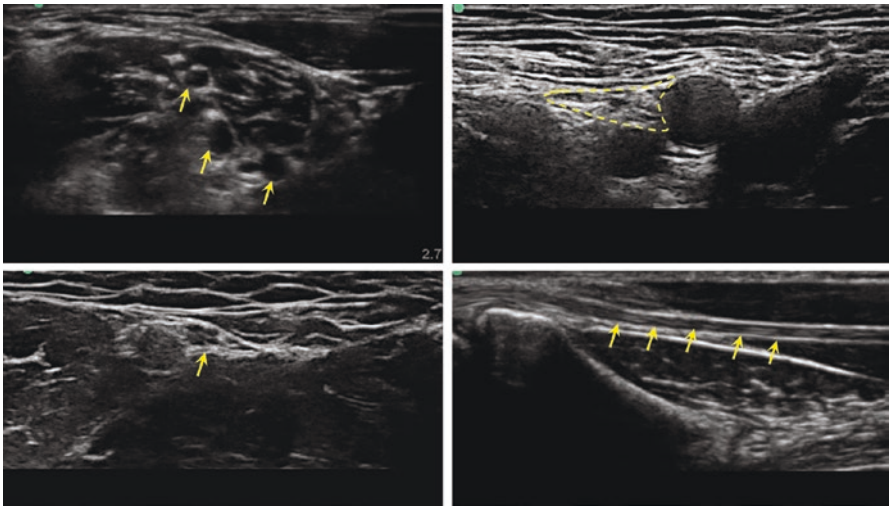

Fig. 1.23 Sonoanatomy of nerves. (Reprinted with permission from Philip Peng Educational Series)

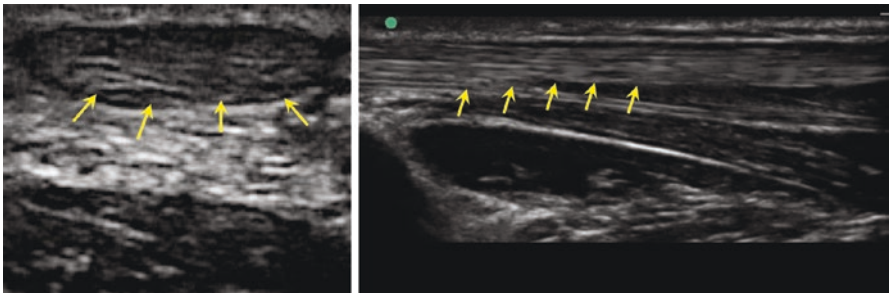

Fig. 1.24 Sonoanatomy of a tendon. (Reprinted with permission from Philip Peng Educational Series)

Artifacts

Reverberation

This is the production of false echoes due to repeated reflections between two interfaces with high acoustic impedance mismatch. The echo from the interface is received by the transducer and displayed on the image. Some of the energy in the returned echo is reflected at the transducer crystals and returns to the reflecting interface as if it was a weak transmitted pulse, returning as a second wave (Fig. 1.25). The time taken for the second wave to arrive is twice that taken by the depth.

This sequence of transmission and reflection can occur many times, with the third wave taking three times as long to return to the transducer and being displayed at three times the depth. These reverberation echoes will be strong because of the high acoustic mismatch.

There are few tricks to reduce reverberation artifact:

1. Increase the amount of gel used
2. Use a standoff pad.
3. Reduce the gain.
4. Adjust the position of the transducer.

Acoustic Shadowing

This appears as an echo-free area behind structures of strongly attenuating tissue. Because of the very high attenuation of the beam at an interface, the transmission is substantially reduced. This artifact can also appear at an interface with large acoustic mismatch such as soft tissue and gas, also at a soft tissue and bone (Fig. 1.26).

Acoustic Enhancement Artifact

This appears as a localized area of increased echo amplitude behind an area of low attenuation. On a scan, it will appear as an area of increased brightness and can commonly be seen distal to fluid-filled structures such as a cyst (Fig. 1.27). This arises due to the application of the time gain compensation (TGC) to areas of low attenuation structure such as fluid. It is caused by the low level of attenuation of the beam as it passes through fluid relative to the greater attenuation of the beam in the adjacent more solid tissue.

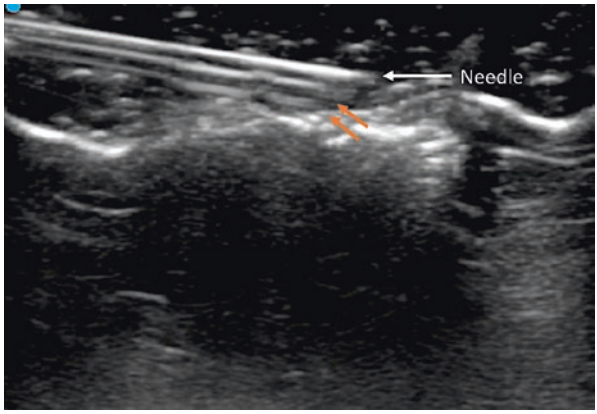

Fig. 1.25 Reverberation artifact. (Reprinted with permission from Philip Peng Educational Series)

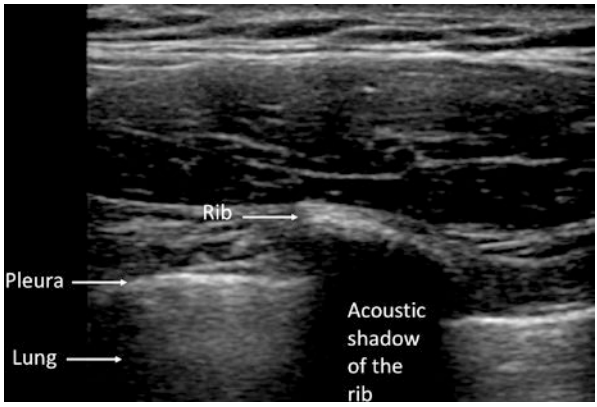

Fig. 1.26 Acoustic shadowing. (Reprinted with permission from Philip Peng Educational Series)

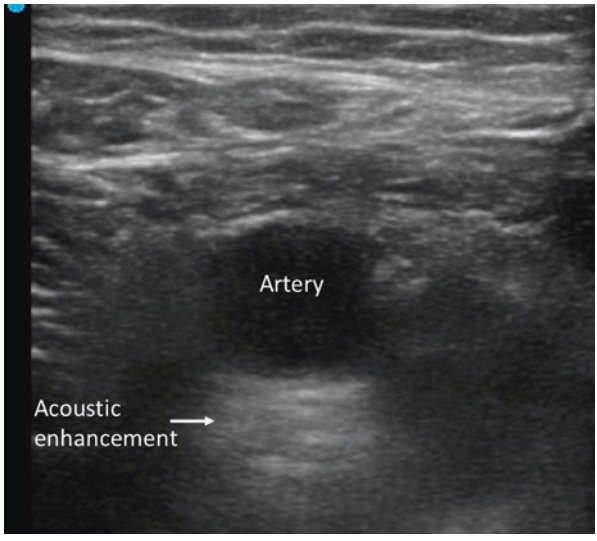

Fig. 1.27 Acoustic enhancement. (Reprinted with permission from Philip Peng Educational Series)

Edge Shadowing

This appears as a narrow hypoechoic shadow line extending down from the edge of a curved reflector (Fig. 1.28). It arises due to refraction of the beam caused by both the curvatures of the rounded edges. When the ultrasound beam races the rounded edge of the structure, reflection will occur, with an angle of incidence equal to the angle of reflection. The outer part of the beam will be totally reflected, but the reminder of the beam passes through the rounded structure and is refracted.

Mirror Imaging Artifact

This artifact results in a mirror image of the structure in an ultrasound display. They arise due to specular reflection of the beam at large smooth interface (Fig. 1.29). An

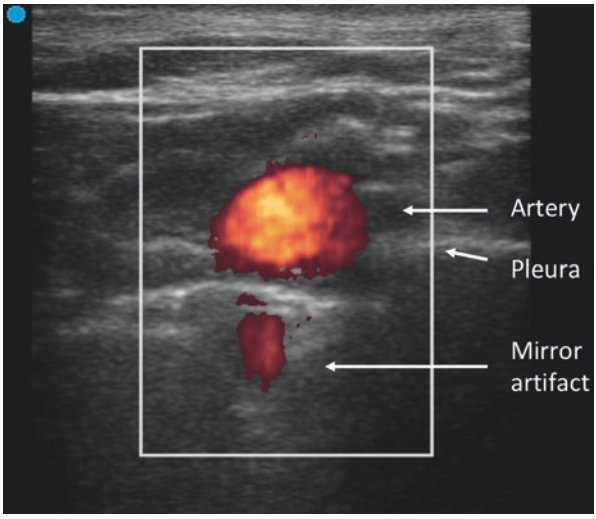

Fig. 1.29 Mirror imaging artifact. (Reprinted with permission from Philip Peng Educational Series)

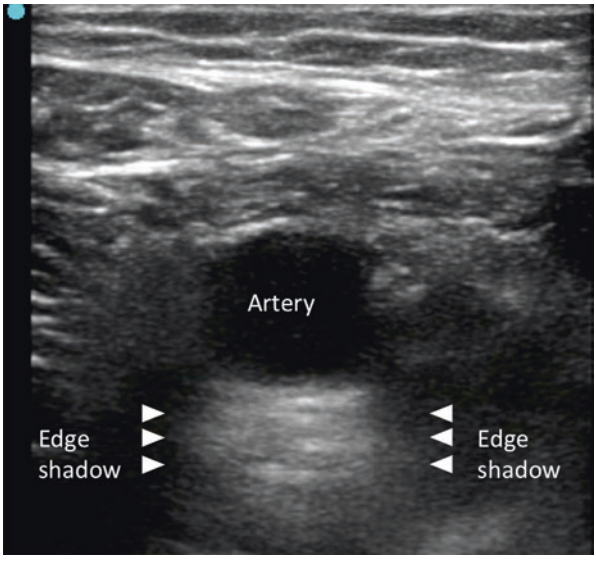

Fig. 1.28 Edge shadowing. (Reprinted with permission from Philip Peng Educational Series)

area close to specular reflector will be imaged twice, once by the original ultrasound beam and once by the beam after it has reflected off the specular reflector. Mirror image artifacts are commonly seen where there is a large acoustic mismatch, such as fluid-air interface. As an example, typically this artifact can occur during the scanning of the subclavian artery on top of the lung (fluid-air interface). It will then have the appearance of a mirror image of the artery within the lung.

Air Artifact

At the transducer skin interface, a large dropout artifact can occur due to a lack of conductive gel and poor transducer to skin contact (Fig. 1.30).

Anisotropy

Anisotropy refers to the angle dependence appearance of a structure (such as tendon) on an image (Fig. 1.31a). When the transducer is perpendicular to the long axis of the object, it results in maximum reception of the signal and optimal image. Tilting the transducing affects the signal and thus the image produced.

This affects the quality of the image because the reflection of sound wave is maximum when the transducer (and the incident waves) is perpendicular to the

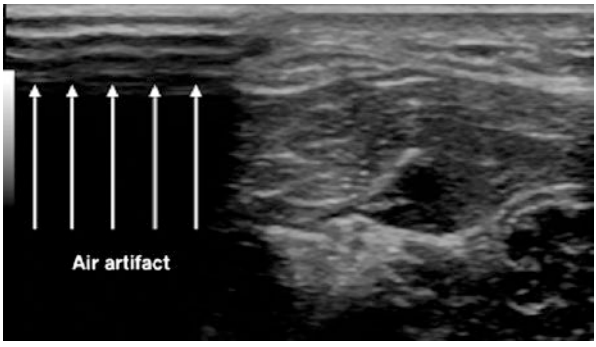

Fig. 1.30 Air artifact. (Reprinted with permission from Philip Peng Educational Series)

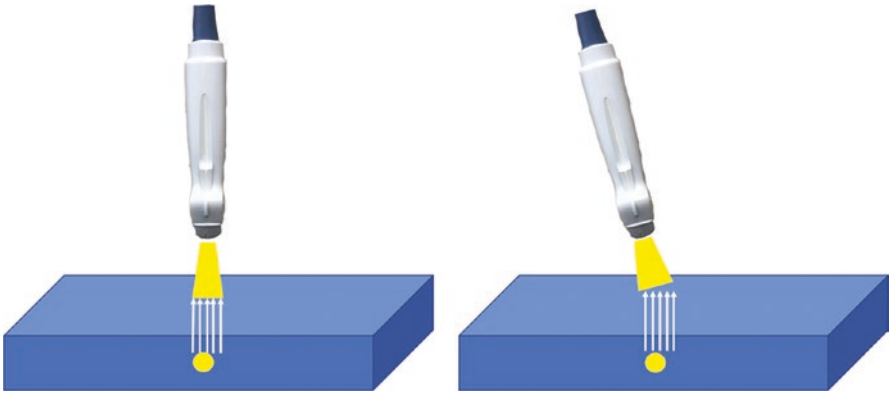

Fig. 1.31a Angle of the ultrasound and the target structure. (Reprinted with permission from Philip Peng Educational Series)

structure (median nerve in this case) under examination (left panel) (Fig. 1.31b). Any change on this incidence angle dramatically reduces the returning echo, causing the structure to "disappear" out of the image (right panel). Manipulation of the transducer (so as to direct the incident beam perpendicular to the structure of interest) and beam-steering can help address anisotropy.

Things to Remember for Optimal Ultrasound Scanning and Performance

Scanning and Positioning Terminology

View and Needle Insertion

Short and long axis is based on the position of the probe with reference to the axis of structure (Fig. 1.32). If the probe is place along the axis of the target structure to be scanned, it is showing the long axis view (Fig. 1.33a).

The approach to insert the needle is described according to the orientation of needle to the plane of ultrasound beam (Fig. 1.33b). If the needle tip and the shaft are inserted in a way such that both are in the ultrasound beam, it is called in-plane. If the axis of needle insertion is right angle to the ultrasound beam, it is out-of-plane.

Transducer Handling

There are four basic transducer handling (mnemonic = "PART") (Fig. 1.34).

- P = Pressure, adjust according to the depth of target for visualization
- A = Alignment, sliding the transducer longitudinally
- R = Rotation, rotating the transducer (clockwise/counterclockwise)
- T = Tilting, tilting or angling the transducer

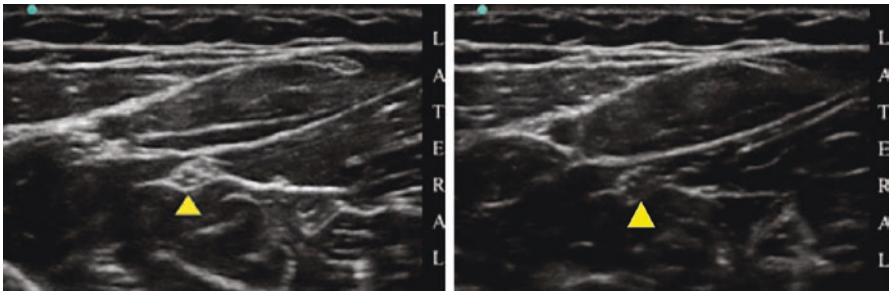

Fig. 1.31b Anisotropy of median nerve. (Reprinted with permission from Philip Peng Educational Series)

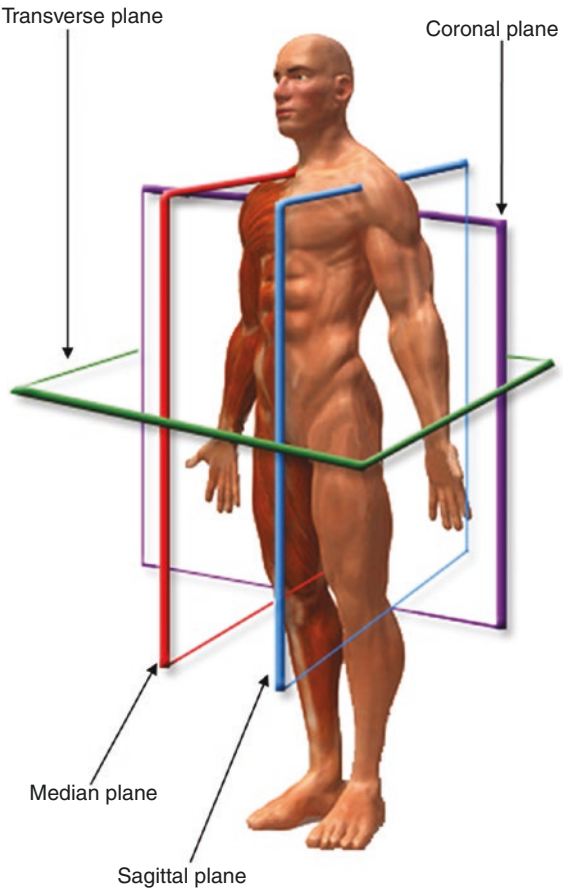

Fig. 1.32 The three different planes. (Reprinted with permission from usra.ca)

Ergonomics

Ergonomics is the study (or science) of the interaction between humans and their working environment. Recent years have witnessed an increasing application of optimal procedural ergonomics in regional anesthesia in an effort to improve outcomes. Poor ergonomics may not only lead to suboptimal performance of a procedure but may contribute to work-related musculoskeletal discomfort.

A sound application of the principles of ergonomics to regional anesthesia and pain management includes the consideration of the following factors:

Positioning and Care of the Patient

Position of patient is important for comfort of patient and for maximal exposure. This position may vary with the type of block being performed. For example, the patient may need a supine position for an upper limb procedure, a prone position for a lower limb procedure, and a sitting position for a neuraxial procedure. Additionally, the position of the limb may be adjusted to assist the procedure.

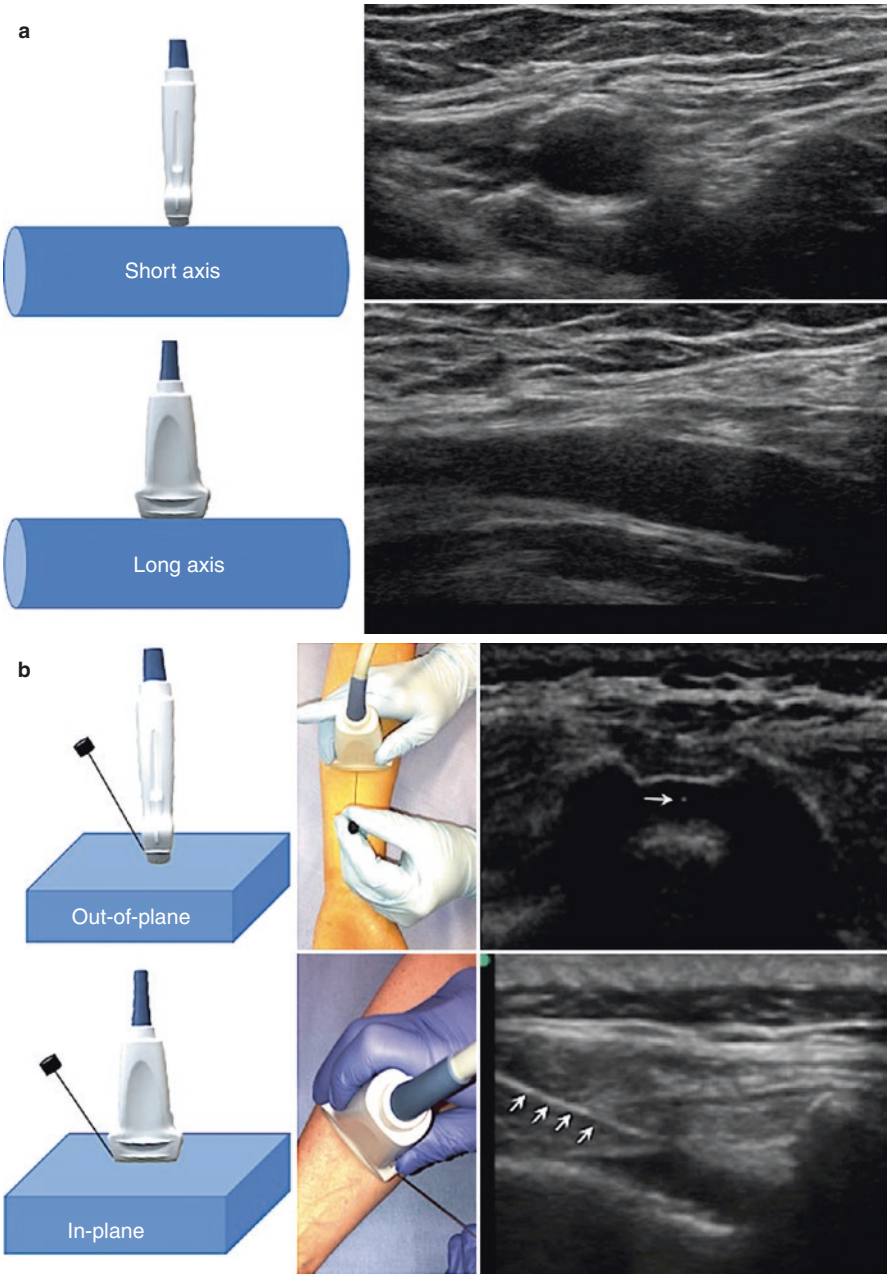

Fig. 1.33 (**a**) Short and long axis. (**b**) In-plane and out-of-plane. (Reprinted with permission from Philip Peng Educational Series)

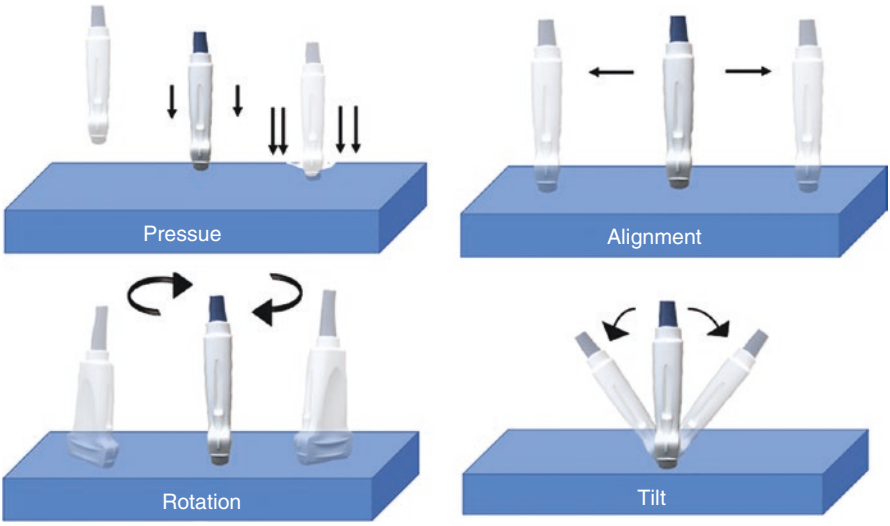

Fig. 1.34 Pressure, alignment, rotation, and tilt. (Reprinted with permission from Philip Peng Educational Series)

Positioning of the Physician

Maintaining a good position with respect to the patient helps to ensure operator comfort and allows optimal procedure performance (Fig. 1.35). This includes the following:

(a) Adjusting the height of patient bed to an appropriate level for the operator.
(b) Assuming a good posture, by choosing to stand or sit down (on a chair).
(c) Performing the procedure from the same target side to avoid reaching over the patient.

Positioning the Equipment

The ultrasound machine is placed in a position so that the operator can view the site of injection and the machine without turning the head. Similarly, the screen of the monitoring equipment must be turned to face the operator during the block to allow a prompt recognition of any significant change of vital signs (Fig. 1.36).

Position of the Assistant

An assistant may be needed both to operate the ultrasound machine and to inject the local anesthetic solution. This may be achieved by standing opposite to the operator and near the ultrasound machine.

Fig. 1.35 Correct and incorrect position of the physician. (Reprinted with permission from Philip Peng Educational Series)

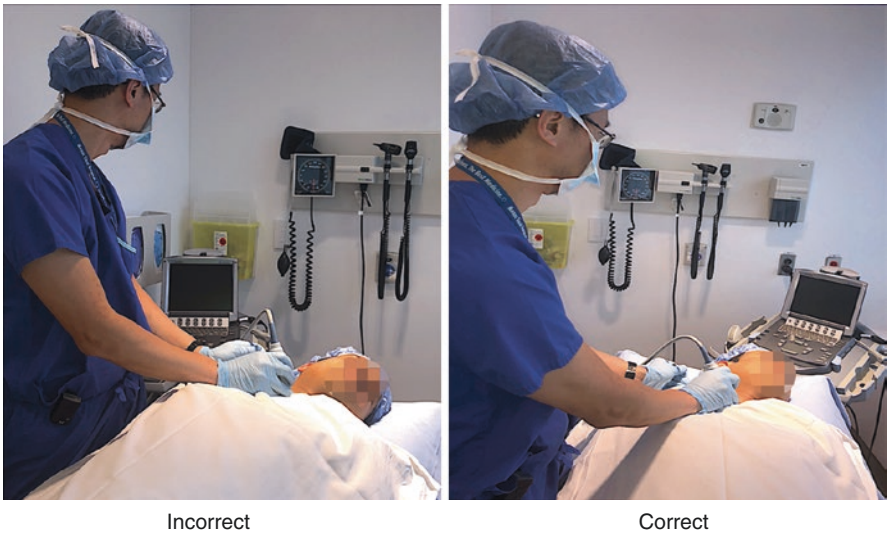

Fig. 1.36 Correct and incorrect position between the operator, patient, and ultrasound machine. (Reprinted with permission from Philip Peng Educational Series)

Fig. 1.37 Correct and incorrect position of holding the ultrasound probe. (Reprinted with permission from Philip Peng Educational Series)

Holding the Probe and Needle Insertion

It is important to have a steady control of the probe position. The probe can be held with 2–3 fingers, and the hand can rest on the body of the patient gently to gain support (Fig. 1.37).

When inserting the needle, make sure your needle is within the field of view of the ultrasound scan, no matter it is in-plane or out-of-plane approach (Fig. 1.38a). Otherwise, the needle is inserted in the wrong plane with reference to the ultrasound field of view and may result in inadvertent tissue puncture (Fig. 1.38b).

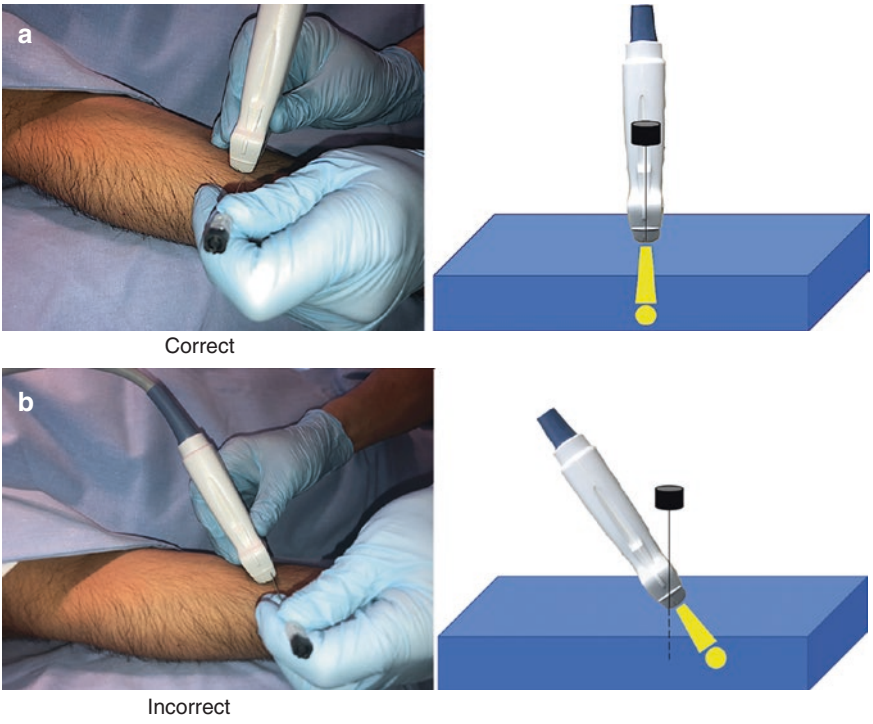

Fig. 1.38 (**a**) Correct angle of insertion of needle. (**b**) Incorrect angle of entry of needle. (Reprinted with permission from Philip Peng Educational Series)

Glossary (Table 1.4)

Table 1.4 Dictionary of terms used in the chapter

Terminology	Definition
Ultrasound	Sound waves of very high frequency (2 MHz or greater)
Absorption	The loss of ultrasound energy when passing through a medium resulting in its conversion to another form of energy such as heat or intracellular mechanical vibration
Acoustic impedance	The resistance to sound transmission through a medium
Acoustic intensity	The concentration of energy in a sound beam; the amount of acoustic power transmitted per unit area
Acoustic power	The amount of acoustic energy generated per unit time
Amplitude	The strength of a sound signal
Artifacts	Display distortions, additions, or errors that can adversely affect ultrasound image acquisition or interpretation
Attenuation	A decrease in amplitude and intensity, as sound travels through a medium. Attenuation occurs with absorption (conversion of sound to heat), reflection (portion of sound returned from the boundary of a medium), and scattering (diffusion or redirection of sound in several directions when encountering a particle suspension or a rough surface)
Axial resolution	The ability to distinguish two structures as separate when the structures are lying close to each other along the same axis as the ultrasound path
Cycle	The combination of one rarefaction and one compression equals one cycle
Diffuse reflection	The reflection that comes off a reflector with an irregular surface
Doppler effect	A change in the frequency of sound as a result of motion between the sound source and the receiver; a positive shift occurs when the source and receiver are approaching each other, and a negative shift occurs when they are moving away from each other
Dynamic range	The ratio of the maximum level of a given parameter to its minimum level; in ultrasound, the dynamic range defines a range of echo intensities that are displayed as a gradient of gray values (minimum value in black and maximum value in white pixels in the final image)
Echogenicity	The degree of brightness of a structure displayed on ultrasound; this is influenced by the amount of beam returning to the transducer (reflection) after encountering the target structure
Enhancement	Increase in reflection amplitude from reflectors that lie behind a weakly attenuating structure, i.e., cysts or solid masses
Frequency	The number of cycles per second; frequency is the inverse of wavelength; the higher the frequency, the shorter the wavelength
Gain	Refers to the amount of amplification of the returning echoes
Gel couplant	A transonic material which eliminates the air interface between the transducer and the animal's skin
Homogenous	Of uniform appearance and texture
Hyperechoic	The image characteristic of a structure that is highly reflective resulting in a brighter displayed image compared to the surrounding structures; the bone and pleura are examples of hyperechoic structures
Hypoechoic	The image characteristic of a structure that is less reflective than the surrounding structure resulting in a darker displayed image compared to the surrounding structures; fluid-filled structures, e.g., vessels and cyst are hypoechoic
Interface	The boundary between two tissue media with different acoustic impedances

(continued)

Table 1.4 (continued)

Lateral resolution	The ability of the system to distinguish two structures as separate when the structures are lying side by side
Longitudinal wave	Movement of particles in the same direction as the direction of the wave propagation
Mechanical probes	Allows the sweeping of the ultrasound beam through the tissues rapidly and repeatedly. This is accomplished by oscillating a transducer. The oscillating component is immersed in a coupling liquid within the transducer assembly. In our case, the coupling fluid is deionized water. It is important that the fluid is bubble free, so that your image is not compromised. Check the water level in the transducer assembly before scanning, and if you see air bubbles, make sure you fill it with the deionized water
M-mode	Is the motion mode displaying moving structures along a single line in the ultrasound beam
Noise	An artifact that is usually due to the gain control being too high
Period	The amount of time required to complete one cycle
Pulsed transducers	Consists of one transducer element which functions as Both the source and receiving transducers
Pulse repetition frequency	The number of pulses occurring in a given time interval; for example, 1 Hz (hertz) is one cycle per second and 10 Hz is ten cycles per second; a lower PRF is required for unambiguous discrimination of structures at deeper imaging depths
Pulse repetition period	Time from the start of one pulse to the start of the next pulse
Pulse duration	The time measured from the start of one pulse to the end of the same pulse
Rayleigh scattering	Scattering of the wave in all directions when the reflector is much smaller than the ultrasound wavelength
Reflection	Mirror-like redirection and return of a propagating sound wave toward the transducer that follows a standard law of reflection; for example, specular reflection results in the reflected angle being equal to the incident angle of the energy propagation
Refraction	A change in the direction of wave propagation when traveling from one medium to another with different propagation speeds according to the Snell's law of refraction
Resolution	The ability to distinguish between two structures that lie close to one another
Reverberation	Multiple reflections commonly seen in the bladder or heart
Scattering	A process by which the ultrasound is forced to deviate from a straight-line reflection and trajectory due to small, localized nonuniformities in the tissue
Shadowing	Created by strong reflectors or attenuating structures, i.e., the bone, gas, calcifications, and air
Speckle	The granular appearance of images and spectral displays that is caused by the interference of echoes from the distribution of scatterers in tissue
Specular reflection	The reflection that comes off a smooth reflector (e.g., a mirror)
Transverse wave	Movement of particles perpendicular to the direction of the wave propagation
Transducers	Convert one form of energy to another. Ultrasound transducers convert electric energy into ultrasound energy and vice versa. Transducers operate on piezoelectricity meaning that some materials (ceramics, quartz) produce a voltage when deformed by an applied pressure and reversely result in a production of pressure when these materials are deformed by an applied voltage

Suggested Reading

Abbas K, Chan V. Basic understanding of ultrasound scanning. In: Peng P, editor. Ultrasound in pain medicine intervention: a practical guide, Philip Peng educational series, vol. I. California: Apple Inc; 2014.

Chin KJ. Needle and transducer manipulation: the art of ultrasound guided regional anesthesia. Int J Ultrasound Appl Technol Periop Care. 2010;1:27–32.

Sehmbi H, Perlas A. Basic of ultrasound imaging. In: Jankovic D, Peng P, editors. Regional nerve blocks in anesthesia and pain therapy. Cham: Springer; 2015.

Greater and Lesser Occipital Nerve

2

Yasmine Hoydonckx and Philip Peng

Introduction

Indication of Blockade

Blockade of the greater and lesser occipital nerves has been implicated in different types of chronic headaches, including primary headaches and secondary headaches (Table 2.1). Patients with these types of headaches often experience good pain relief by targeting the occipital nerves.

The basis of how occipital nerve block works in the primary headache is likely related to the convergence of the functional connection between the sensory inputs from the occipital segments with the nuclei of the trigeminal nociceptive system (the trigeminocervical complex). From there, the neural circuit connects further to thalamus and cortex. Temporary suppression of the inputs from the greater occipital nerve (GON) may lead to modulation of central nociceptive pathways and reducing central sensitization.

Traditionally, the GON block is performed with blinded approach relying on the anatomic landmarks at the level of the superior nuchal line. This approach poses a higher risk to injection in the occipital artery and/or block failure. Complication rates of 5–10% have been reported, including dizziness, blurred vision, and syncope. Use of ultrasound has been shown not only to reduce the risks but also to improve the block efficacy.

Y. Hoydonckx
Department of Anesthesia and Pain Medicine, University of Toronto and Toronto Western Hospital, University Health Network, Toronto, ON, Canada

P. Peng (✉)
Department of Anesthesia and Pain Management, Toronto Western Hopsital and Mount Sinai Hospital, University of Toronto, Toronto, Ontario, Canada
e-mail: Philip.peng@uhn.ca

P. Peng et al. (eds.), *Ultrasound for Interventional Pain Management*,
https://doi.org/10.1007/978-3-030-18371-4_2

Table 2.1 Indications of occipital nerve blocks in headache

	Specific types of headache
Primary	Migraine, cluster headaches, post-concussion headache
Secondary	Cervicogenic headache, occipital neuralgia

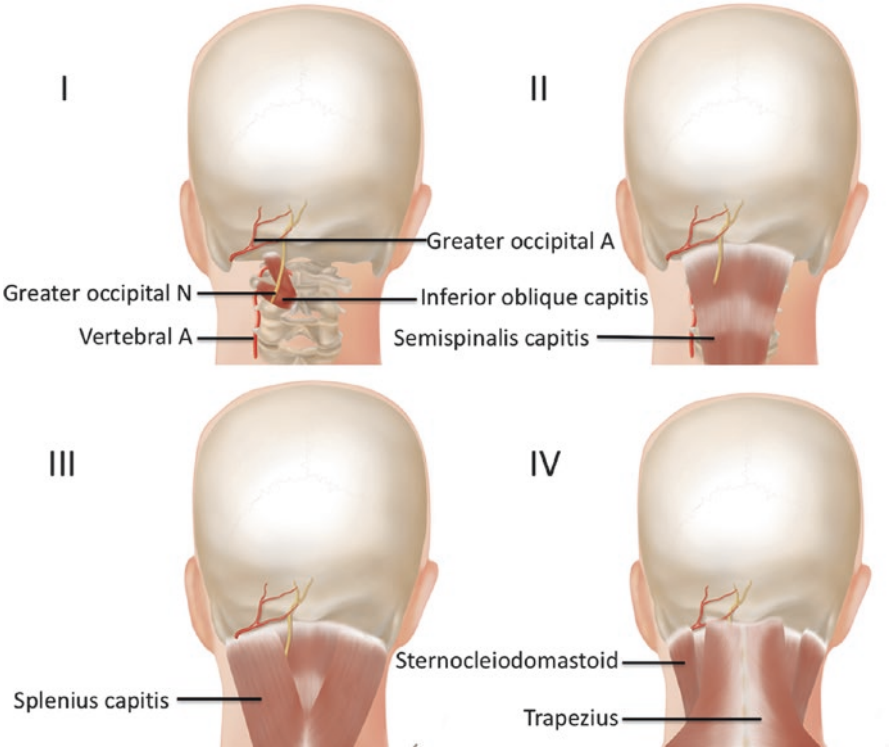

Fig. 2.1 Fours layers of muscles relevant to the greater occipital nerve. N and A-nerve and artery. (Reprint with permission from Philip Peng Educational Series)

Anatomy

The greater occipital nerve (GON) originates from the medial branch of the dorsal ramus of the C2 spinal nerve, with contributions from the C3 dorsal ramus.

The GON exits below the posterior arch of the second cervical vertebra, curves around the inferior oblique capitis (IOC) muscle, and travels cephalad in an oblique trajectory between the inferior oblique capitis and semispinalis capitis (SSC) muscle. At this site, the GON is susceptible to potential entrapment. The GON then perforates the trapezius muscle and ascends medial to the occipital artery to innervate the posterior cutaneous aspect of neck and scalp (Fig. 2.1).

The lesser occipital nerve (LON) is the most cephalad branch of the superficial cervical plexus beneath the sternocleidomastoid muscle. It is formed by fibers of the

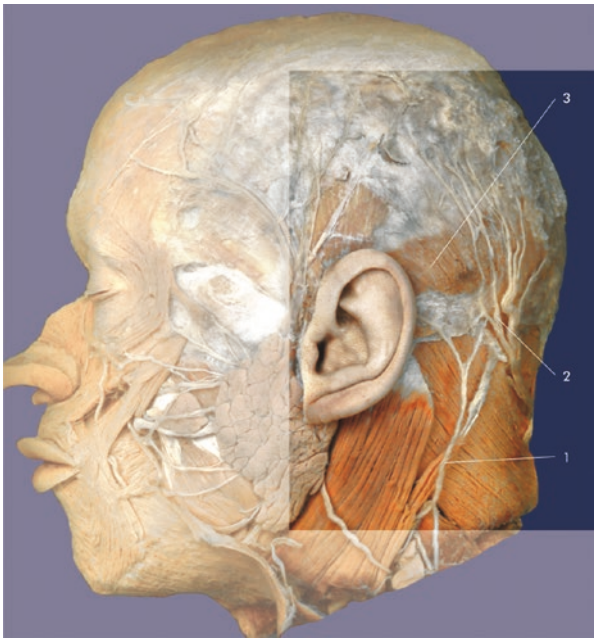

Fig. 2.2 (1) Lesser occipital nerve, (2) greater occipital nerve and occipital artery, and (3) occipital muscle. (Reprinted with permission from Danilo Jankovic)

ventral rami of C2 and C3 and curves around its posterior border to run cranially to the parieto-occipital area where it splits in its terminal branches to innervate the lateral part of the occiput (skin behind and above the ear) (Fig. 2.2).

Patient Selection

The diagnosis of a specific headache type can be made according to the International Head Society (IHS) classification. The occipital nerve block plays a diagnostic role in the diagnosis of occipital neuralgia and cervicogenic headache. For the other aforementioned headaches, the nerve block can be considered in patient's failure to respond to conservative management.

Ultrasound Scanning

The Greater Occipital Nerve: Two Different Target Locations

Proximal Approach at Level of C2

- Position: Prone with head and neck flexed
- Probe: Linear, 12–18 MHz

The key landmarks are the spinous process of C2 and the inferior oblique capitis muscle.

Scan 1: Occipital protuberance (probe in transverse orientation (Fig. 2.3).

Scan 2: Spinous process of C2. It showed a bifid bone structure below the occiput (Fig. 2.4).

Scan 3: The transducer is moved laterally to visualize the inferior oblique capitis (IOC) muscle and semispinalis capitis (SSC) muscle; to maximize the image of this muscle, the lateral end of the probe is rotated slightly in a cranial direction to bring the transducer parallel to the long axis of the muscle (Fig. 2.5). With this movement, the C2 lamina appears boat-shaped, and IOC is cradled within it. The plane between the IOC and SSC is visualized. Greater occipital nerve (GON) is sandwiched between the IOC and SSC muscles. LON-lesser occipital nerve, SCM-sternocleidomastoid.

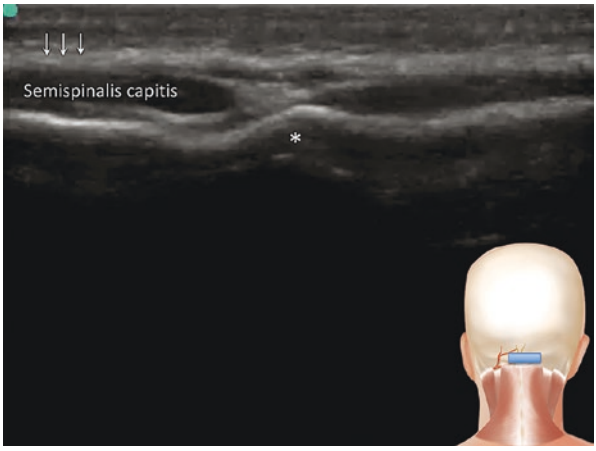

Fig. 2.3 The scan at the occipital protuberance (*). The arrows indicated the superficial fascia of the scalp. The position of the ultrasound probe is shown in the picture in the left lower corner. (Reprinted with permission from Philip Peng Educational Series)

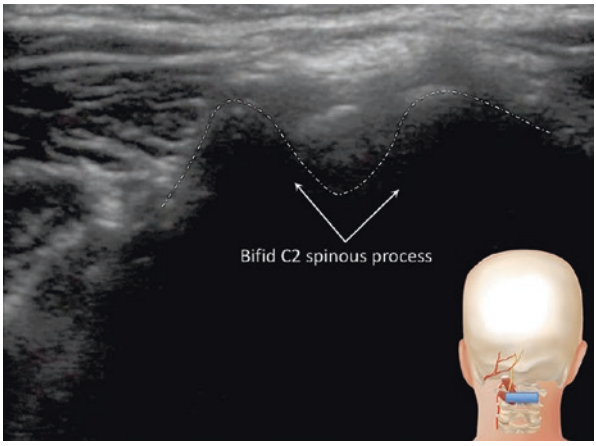

Fig. 2.4 Scan at the C2 level. (Reprinted with permission from Philip Peng Educational Series)

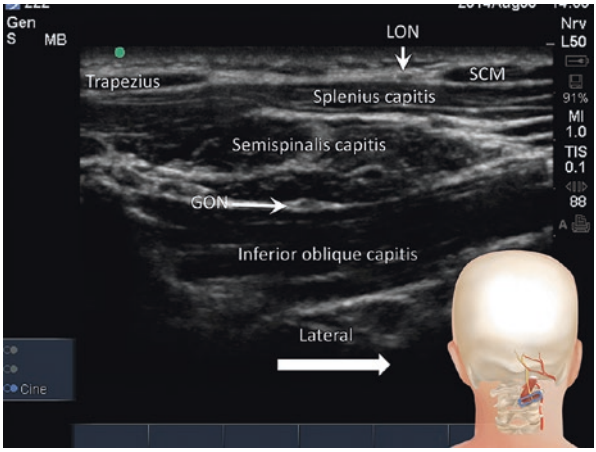

Fig. 2.5 Ultrasound scan at C2 level with the lateral end of the transducer tilted toward C1 lateral mass. (Reprinted with permission from Philip Peng Educational Series)

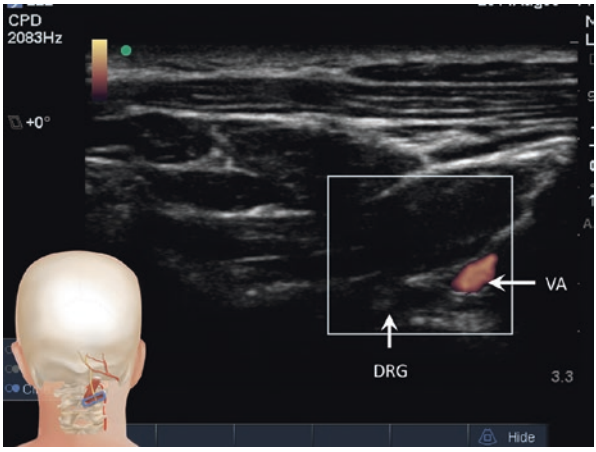

Fig. 2.6 By moving the probe further in the lateral direction as in Fig. 2.5 and applying the Doppler, it revealed the vertebral artery (VA) and the dorsal root ganglion (DRG). (Reprinted with permission from Philip Peng Educational Series)

Scan 4: Doppler scan on the lateral side reveals the vertebral artery (VA) and dorsal root ganglion (DRG) (Fig. 2.6).

Distal Approach at Level of Occiput

- Position: Prone/sitting
- Probe: Linear, 12–18 MHz

The key landmark is the superior nuchal line and occipital protuberance.

Scan 1: Upper sonograph shows the transverse view at superior nuchal line (Fig. 2.7a).

Scan 2: The lower sonograph shows the transducer moved laterally until the greater occipital artery is visualized (Fig. 2.7b). The GON is not commonly

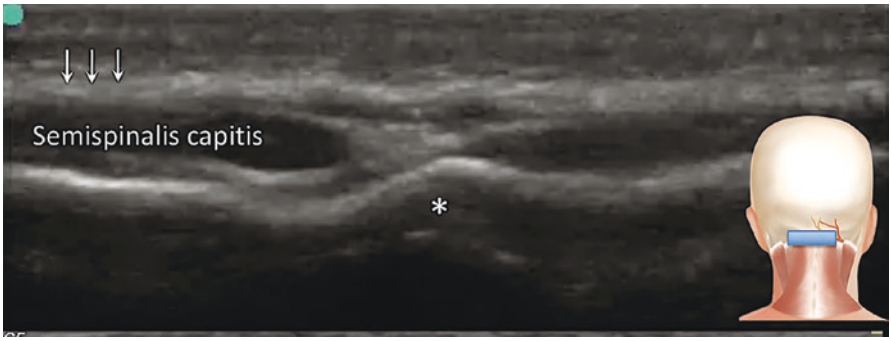

Fig. 2.7a Scan at occipital protuberance (*) and arrows indicated the superficial fascia. (Reprinted with permission from Philip Peng Educational Series)

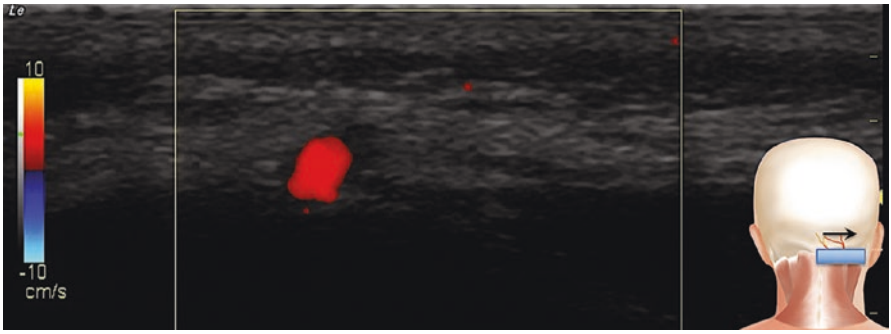

Fig. 2.7b Doppler showed the occipital artery which is in the same fascia plane with the greater occipital nerve. (Reprinted with permission from Philip Peng Educational Series)

visualized as it is usually divided into small branches. However, the visualization of the artery and the plane it is in help to direct the needle to the lateral side of the artery.

The Lesser Occipital Nerve

- Position: Prone/sitting
- Probe: Linear, 12–18 MHz

The key landmark is the posterior border of the sternocleidomastoid muscle, caudal to the mastoid.

Scan 1: The probe is moved cranially and caudally along the posterior border of sternocleidomastoid (SCM) until a nerve structure is identified (Fig. 2.8).

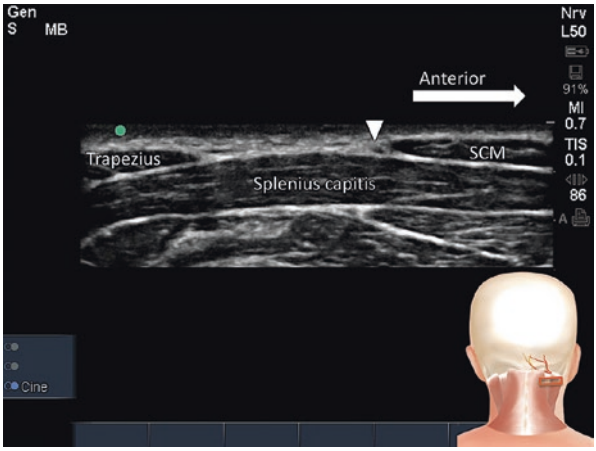

Fig. 2.8 Sonography showed the lesser occipital nerve. SCM-sternocleidomastoid. (Reprinted with permission from Philip Peng Educational Series)

Procedure

- Equipment: 22G 3.5-inch needle
- Drugs: Bupivacaine 0.25% 4 mL with 40 mg Depo-Medrol

Proximal Approach at Level of C2

- A 25G needle infiltrates the skin with 2% lidocaine and then advances in an in-plane technique from lateral to medial (more experienced practitioner may choose out of plane) toward the plane between the inferior oblique capitis muscle and semispinalis capitis muscle (Fig. 2.9).
- Needle tip position is confirmed by using hydrodissection with normal saline (Fig. 2.9).
- Check for absence of vascular structures using Doppler.
- Aspiration is negative prior to injection of therapeutic medication.
- The spread of the injectate is visualized as it surrounds the GON.

Distal Approach at Level of Occiput

- A 25G needle is inserted in an in-plane technique and used to numb the skin with lidocaine 2%.
- The same 25G needle is advanced toward the fascia plane with the greater occipital artery and greater and lesser occipital nerve.
- Aspiration is negative prior to injection of 2 mL of therapeutic medication (4 mL of bupivacaine 0.25% with 40 mg methylprednisolone), medial from the occipital artery.